Inorganic Chemistry

pubs.acs.org/IC Article

Catalytic Urea Synthesis from Ammonium Carbamate Using a Copper(II) Complex: A Combined Experimental and Theoretical Study

Danielle S. Hanson, Yigui Wang, Xinrui Zhou, Erik Washburn, Merve B. Ekmekci, Donovan Dennis, Amay Paripati, Dequan Xiao,* and Meng Zhou*

Cite This: *Inorg. Chem.* 2021, 60, 5573−5589 Read Online

ACCESS | Metrics & More | Article Recommendations | Supporting Information

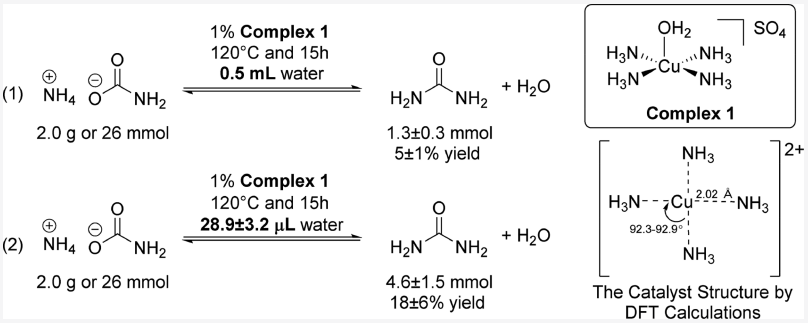

ABSTRACT: The synthesis of urea fertilizer is currently the largest CO_2 conversion process by volume in the industry. In this process, ammonium carbamate is an intermediate *en route* to urea formation. We determined that the tetraammineaquacopper(II) sulfate complex, $[Cu(NH_3)_4(OH_2)]SO_4$, catalyzed the formation of urea from ammonium carbamate in an aqueous solution. A urea yield of up to 18 ± 6% was obtained at 120 °C after 15 h and in a high-pressure metal reactor. No significant urea formed without the catalyst. The urea product was characterized by Fourier transform infrared (FT-IR), powder X-ray diffraction (PXRD), and quantitative $^1H\{^{13}C\}$ NMR analyses. The $[Cu(NH_3)_4(OH_2)]SO_4$ catalyst was then recovered at the end of the reaction in a 29% recovery yield, as verified by FT-IR, PXRD, and quantitative UV−vis spectroscopy. A precipitation method using CO_2 was developed to recover and reuse 66 ± 3% of Cu(II). The catalysis mechanism was investigated by the density functional theory at the B3LYP/6-31G** level with an SMD continuum solvent model. We determined that the $[Cu(NH_3)_4]^{2+}$ complex is likely an effective catalyst structure. The study of the catalysis mechanism suggests that the coordinated carbamate with $[Cu(NH_3)_4]^{2+}$ is likely the starting point of the catalyzed reaction, and carbamic acid can be involved as a transient intermediate that facilitates the removal of an OH group. Our work has paved the way for the rational design of catalysts for urea synthesis from the greenhouse gas CO_2.

INTRODUCTION

The production of urea, a major fertilizer[1] and a cosmetic ingredient,[2] is perhaps the largest industrial process that converts CO_2 (a greenhouse gas) into a commodity chemical.[3−5] According to the International Fertilization Association, the annual production of urea was 157 million tons in 2010.[6] Anthropogenic CO_2 in the atmosphere is linked to ocean acidification and global warming.[4] Therefore, urea production from CO_2 is beneficial for the reduction of carbon emissions[4] and the sustainable production of carbon-based chemicals.

Urea is made in the industry using CO_2 and ammonia supercritical fluid without a catalyst (i.e., via the Bazarov process).[1,7] The critical point of CO_2 is at 73.8 bar and 30.9 °C,[8] and the critical point of NH_3 is at 113 bar and 132 °C.[9] Hence, the Bazarov process requires a high temperature and pressure,[1] e.g., up to 250 bar and 227 °C.[5] Meanwhile, this process involves two steps. First, CO_2 combines with ammonia to form ammonium carbamate in a fast and exothermic reaction (ΔH^0 = −36 kcal/mol).[1,5] Second, ammonium carbamate is converted into urea in a slow and endothermic reaction (ΔH^0 = 7.6 kcal/mol).[1,5] Governed by these thermodynamic constraints, the industrial synthesis of urea cannot fully consume the reactants (CO_2 and ammonia), which are thus recycled using a "stripping process" to increase the yield. Fréjacques, Inoue, and others studied the chemical equilibria of urea synthesis from 1948 to 1998.[1,6,10−16] In 1972,

Received: November 24, 2020
Published: April 7, 2021

https://doi.org/10.1021/acs.inorgchem.0c03467
Inorg. Chem. 2021, 60, 5573−5589

Scheme 1. CO_2 Capture by Ammonia at 0 °C and in an Organic Solvent

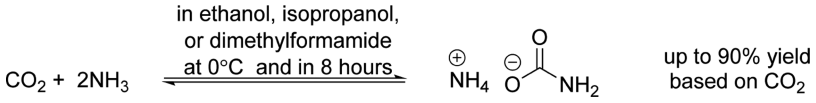

Scheme 2. CuO-Catalyzed Urea Formation without Any Solvent over 3 Days

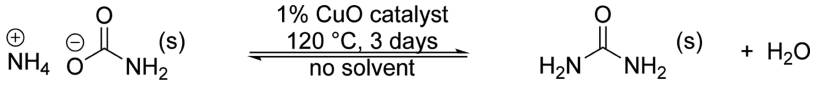

Scheme 3. Urea Formation Catalyzed by Complex 1, Tetraammineaquacopper(II) Sulfate, Using Water as the Solvent in 0.5 mL (eq 1) or 28.9 μL (eq 2)[a]

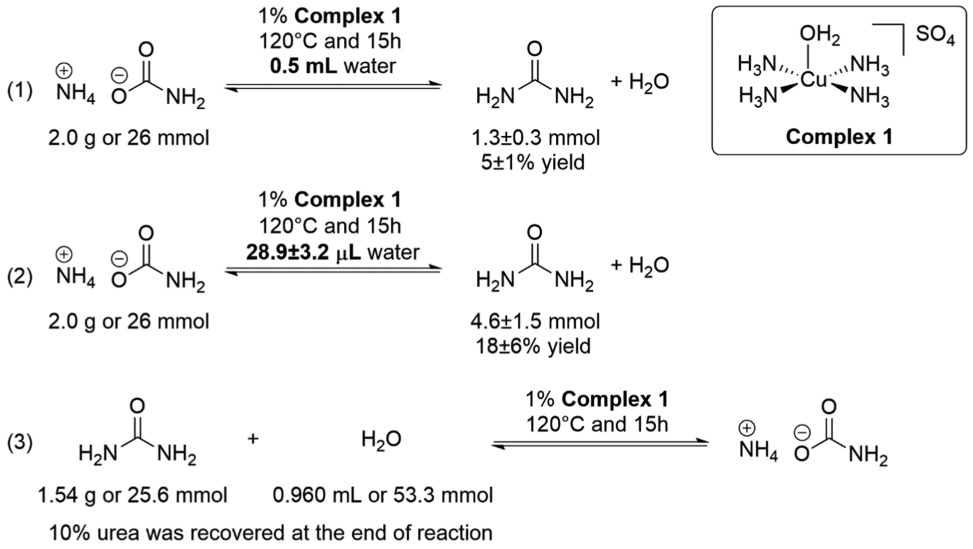

[a]5-Coordinate solid-state structure of **Complex 1** is shown and the reversed reaction of urea formation is shown in eq 3.

Inoue et al. reported[15] that the equilibrium constants went through a maximum of 2.593 at the supercritical conditions of 178 bar and 196.5 °C for urea synthesis starting from CO_2 and NH_3. Urea was analyzed by drying and weighing, and NH_3 and CO_2 were analyzed via titration with H_2SO_4 and $Ba(NO_3)_2$, respectively.

Regarding the reaction mechanism of the uncatalyzed Bazarov process, theoretical studies[7] were conducted by Tsipis et al., showing that an addition−elimination−addition mechanism is favored over an addition−addition−elimination mechanism or a concerted mechanism. The authors also studied the effects of water and ammonia, respectively, on urea formation via density functional theory (DFT) calculations. The calculations were performed in the gas phase and without a continuum solvent model, and no metal catalyst was studied.

Designing active catalysts for urea formation is the key to the industrial synthesis of urea under mild conditions and with high yields. Though a few catalysts[3,5,17−19] have been reported for urea synthesis in the laboratory, no catalyst has been employed in the industry.[1] Thus, it is necessary to develop novel, robust, and active catalysts that are promising for industrial applications. Notably, in 2011, Barzagli et al. reported[5] that urea can be synthesized in two steps (Schemes 1 and 2) using a CuO solid catalyst. Manaka et al. reported[19] in 2020 that an organobase, 1,8-diazabicyclo[5.4.0]undec-7-ene (DBU), catalyzed the urea synthesis from ammonium carbamate in a dimethyl sulfoxide solvent. However, both reactions require 72 h, and a 20% catalyst loading was used to achieve a 35% yield for the DBU-catalyzed reaction. These two methods were developed based on the Bazarov process, which uses CO_2 as the source of carbon (Schemes 1 and 2).[1] Alternatively, C−H activation[20−22] reactions can be used to synthesize urea derivatives from organic compounds, instead of CO_2. In 2017, Krishnakumar et al. reported[23] the synthesis of urea derivatives via the formyl C−H activation of *N*,*N*′-dimethylformamide, as catalyzed by a ruthenium pincer complex. In 2018, Lane et al. reported[24] an oxidative C−N coupling reaction[25] to synthesize urea derivatives from methanol, catalyzed by an iron pincer complex.

In the report by Barzagli et al., CO_2 was initially captured by ammonia in an organic solvent at 0 °C for 8 h (Scheme 1). A CO_2-capturing efficiency of up to 93% was achieved, and ammonium carbamate formed in a 90% yield based on CO_2.

In the second step for converting ammonium carbamate to urea, a copper(II) oxide solid catalyst was used. The solid-state reaction was conducted using 8 g of ammonium carbamate and 1% of CuO without any solvent. Over 3 days under 120 °C and with the pressure close to 14 bar, the reaction gave urea at a 54% yield (Scheme 2). Since ammonium carbamate solid is under a heterogeneous equilibrium[1,5] with CO_2 and ammonia gases, a high-pressure stainless steel reactor was used to perform the reaction in a closed system. The product urea was characterized by ^{13}C NMR spectroscopy, and its yield was calculated based on the weight of the crude product without any purification. In 2016, the same group described the

https://doi.org/10.1021/acs.inorgchem.0c03467
Inorg. Chem. 2021, 60, 5573−5589

Table 1. Urea Formation Catalyzed by Tetraammineaquacopper(II) Sulfate[a]

entry	catalyst loading (%)	temperature (°C)	water	time (h)	turnovers	urea yield (%)
1[a]	**1**	**120**	**0.5 mL**	**15**	**5**	**5**
2[a]	1	120	none	15	0	<1
3	1	120	5 mL	15	0	<1
4[b]	**1**	**120**	**28.9 ± 3.2 μL**	**15**	**18**	**18 ± 6**
5[c]	1	120	115 μL	15	1.5	1.5
6	1	90	0.5 mL	15	0	<1
7[d]	1	120	0.5 mL	15	5	5
8	0.2	120	0.5 mL	15	40	8
9	0.2	120	0.5 mL	30	20	4
10	5	150	none	1	2.6	13
11	1	150	none	1	5	5
12[e]	1	150	none	1	8	8
13	1	150	0.1 mL	1	5	5
14	1	150	0.5 mL	15	6	6
15	0.2	150	none	5	60	12
16	**0.2**	**150**	**none**	**17**	**75**	**15**
17	0.2	150	none	24	75	15

[a]Reaction conditions: the catalyst loading is based on the 26 mmol or 2.0 g of ammonium carbamate; the reaction was conducted in a 22 mL Hastelloy high-pressure metal reactor, under air, using **Complex 1**, tetraammineaquacopper(II) sulfate, as the catalyst, and with 2.0 g of ammonium carbamate as the starting material, unless specified otherwise; the yield of urea was measured using quantitative $^{1}H\{^{13}C\}$ NMR spectroscopy with benzene as an internal standard; the turnovers were calculated by dividing the yield of urea by the catalyst loading ([a]repeated twice; [b]repeated thrice). [b]Three drops of water from a 1 mL plastic syringe and a gauge 22 needle gave 28.9 ± 3.2 μL, with an average over seven measurements. [c]The reaction was conducted on a large scale using 8.0 g or 104 mmol of ammonium carbamate to fill up the 22 mL metal reactor; [d]$CuSO_4 \cdot 5H_2O$ was the catalyst; [e]with CO_2 at 300 psi, measured at 150 °C. The key results are highlighted in bold.

detailed characterizations of a variety of byproducts, such as ammonium bicarbonate, using ^{13}C NMR spectroscopy.[3]

Inspired by the effectiveness of CuO as a catalyst for urea formation, we speculated that CuO could be unstable and transform into water-soluble copper(II)−ammonia complexes due to their high formation constants: up to 2.08×10^{13} for $[Cu(NH_3)_4]^{2+}$.[26−29] Hence, we focused on the stable and well-defined tetraammineaquacopper(II) sulfate complex, $[Cu(OH_2)(NH_3)_4]SO_4$ (**Complex 1**), as the catalyst for urea synthesis. In the mechanistic study by DFT calculations, we studied the conversion of ammonium carbamate into urea in water using **Complex 1** as the catalyst.

In the following sections, we will first demonstrate an effective water-soluble catalyst, **Complex 1**, for urea formation from ammonium carbamate. The results are compared to control experiments without a catalyst and to reactions catalyzed by CuO. Then, we will use ab initio quantum chemistry calculations to reveal the mechanism of urea formation from ammonium carbamate, catalyzed by **Complex 1**. At the B3LYP/6-31G** + SMD-water level of theory, the calculations suggested that the thermodynamically stable $[Cu(NH_3)_4]^{2+}$ was likely the resting state of the catalyst, which is consistent with the established coordination chemistry of the copper(II)−ammonia system.[26,27,29−34]

RESULTS AND DISCUSSION

Urea Formation Catalyzed by the Tetraammineaquacopper(II) Sulfate Complex. We tested the tetraammineaquacopper(II) sulfate complex (i.e., **Complex 1**) as the catalyst for urea formation in water. Details of the synthesis and purification of **Complex 1** are described in the Experimental Procedure section. Using water as the solvent in 0.5 mL and **Complex 1** as the catalyst with a 1% loading, urea formed at a 5% yield after 15 h and at 120 °C (eq 1 in Scheme 3 and entry 1 in Table 1). The key results in Table 1 are highlighted in bold. Five catalyst turnovers were obtained. The turnovers were calculated by dividing the yield of urea by the catalyst loading. The pressure of the reaction was 50 psi at 120 °C. In a control experiment without **Complex 1**, no urea formed under otherwise identical conditions (entry 1 in Table 2). Without water (entry 2 in Table 1), no urea formed under otherwise identical conditions to the entry 1 reaction in Table 1. Additional control experiments without **Complex 1** and under various reaction conditions are described in Table 2. Despite the low turnover number and the yield of the catalytic urea synthesis shown in eq 1 in Scheme 3, the results indicate that the reaction can be catalyzed by a well-defined and water-soluble metal complex. Remarkably, a significant amount of urea was formed in 0.5 mL of water. Water is a side product in reversible urea formation and could shift the equilibrium to the reactant side. To determine whether the yield in urea synthesis was limited by its reversed reaction, catalytic urea hydrolysis was studied (eq 3 in Scheme 3). Urea in 25.6 mmol, the same amount as that of ammonium carbamate in eq 1, reacted with water in 0.960 mL or 53.3 mmol in the presence of **Complex 1** under otherwise identical conditions to those described in eq 1 in Scheme 3. Water in 53.3 mmol was used because, in the

Table 2. Control Experiments for Urea Formation in the Absence of a Cu(II) Catalyst[a]

entry	temperature (°C)	water	time (h)	urea yield (%)
1	120	0.5 mL	15	<1
2*	150	none	1	<1
3	150	0.1 mL	1	<1
4	120	28.9 ± 3.2 μL	15	3

[a]Reaction conditions: in the absence of a copper catalyst, under air, in a 22 mL Hastelloy high-pressure metal reactor, and with 2.0 g or 26 mmol of ammonium carbamate starting material; analyzed by $^{1}H\{^{13}C\}$ NMR spectroscopy; *repeated twice.

https://doi.org/10.1021/acs.inorgchem.0c03467
Inorg. Chem. 2021, 60, 5573−5589

forward reaction (eq 1 in Scheme 3), 0.5 mL of water solvent corresponds to 27.8 mmol, and 25.6 mmol of ammonium carbamate would produce an equimolar amount of water if the forward reaction had gone to completion, giving a combined 53.4 mmol of water. At the end of the reaction, only 10% urea was recovered, which suggests that the equilibrium yield of urea synthesis cannot exceed 10% at 120 °C starting with 0.5 mL of water, as in eq 1. Even at an elevated temperature of 160 °C, Piotrowski et al. reported that the equilibrium yield of urea was limited to 41.2% with a molar ratio of 2.5:1:1 for NH_3/H_2O/CO_2.[11] An equilibrium yield measured at below 160 °C was rarely reported.[1,11]

No copper(II) biuret (λ_{max} = 540 nm)[35] was detected by a UV−vis analysis at the end of the reaction. Only a 620 nm absorption that is consistent with a copper ammonia complex was detected.[26,38] For an NMR analysis, the water side product was removed under vacuum. Proton $^1H\{^{13}C\}$ NMR analysis (^{13}C-decoupled proton NMR analysis) in DMSO-d_6 (deuterated dimethyl sulfoxide) was used to identify urea at 5.49 ppm. An internal standard, benzene, was added at the end of the reaction to quantify the urea. Details of the NMR and UV−vis analyses are described in the Experimental Procedure section. Due to the complexity of the powder X-ray diffraction (PXRD) spectrum of the crude product, the urea sample could not be characterized via PXRD analysis without purification.

To perform the PXRD analysis, we purified and isolated the urea by extraction: dissolving the crude product in methanol, followed by centrifugation and solvent removal (see the Experimental Procedure section for details). Urea was isolated in 90 ± 10% purity via quantitative $^1H\{^{13}C\}$ NMR analysis. The purified urea was confirmed by Fourier transform infrared (FT-IR) and PXRD spectroscopy. No significant biuret was detected by the PXRD analysis.[36] In this purification method, **Complex 1** is insoluble in methanol and was separated from the methanol liquid phase. The unreacted starting material, ammonium carbamate, is soluble in methanol. However, it decomposes rapidly to CO_2 and ammonia when the methanol solvent is removed under vacuum and at 45 °C, as illustrated by the reversible reaction shown in Scheme 1 (see the Experimental Procedure section for details). The PXRD analysis could not reliably detect the potential side product, ammonium bicarbonate, which was previously observed using $^{13}C\{^1H\}$ NMR spectroscopy.[3,5,37] The most intense reflection of ammonium bicarbonate overlaps with an intense reflection of **Complex 1**. The attempt to detect ammonium bicarbonate using PXRD analysis is detailed in the Powder X-ray Analyses of Urea and Biuret section.

Complex 1 was recovered at the end of the reaction (entry 1 in Table 1) and was characterized by FT-IR and PXRD. **Complex 1** is insoluble in methanol and was separated, via centrifugation, from ammonium carbamate and urea, which are soluble in methanol. **Complex 1** was separated from an impurity, a white solid, by suspending the blue, fine particles of **Complex 1** in methanol. **Complex 1** was recovered in a 29% yield, which was measured by quantitative UV−vis analysis with λ_{max} = 605 nm.[26,38] The catalyst can be recovered in 70% by thoroughly removing water before dissolving the reaction mixture in methanol, which is described in the Experimental Procedure section. The insoluble white solid cannot be identified by powder X-ray diffraction: no crystalline reflections can be detected. It is present in small quantities (2−19 mg) and did not reproducibly form. Details of the catalyst recovery are described in the Experimental Procedure section. The FT-IR analysis revealed that the N−H stretching[39] (3309, 3238, and 3168 cm^{-1}), bending[39] (1635 and 1278 cm^{-1}), and rocking[39] (730 cm^{-1}) modes and the S−O stretching mode[40] (1060 cm^{-1}) of the recovered sample matched those of **Complex 1**. The PXRD reflections of the recovered sample also matched those of **Complex 1**, with the most intense reflections found at 14.4, 16.7, 22.0, 25.4, 29.1, 30.4, and 42.8° 2θ.

For a practical method to recover Cu(II) without using methanol, a CO_2 precipitation method was developed based on the following eq 1 for the formation of basic copper carbonate ($Cu_2CO_3(OH)_2$) in water.[41] We envisioned that $Cu_2CO_3(OH)_2$, a cyan precipitate, could be formed by CO_2 instead of Na_2CO_3 based on eq 2, where an NH_3 ligand may dissociate and serve as a base to neutralize H_2CO_3 (CO_2 + H_2O). Both equations are balanced. The byproduct $(NH_4)_2SO_4$, in an equimolar amount to copper, is a common nitrogen fertilizer that can be used in a mixture with urea.[42]

$$\text{known reaction: } 2Cu(NO_3)_2 + 2Na_2CO_3 + H_2O \rightarrow Cu_2CO_3(OH)_2 + CO_2 + 4NaNO_3 \quad (1)$$

$$\text{proposed reaction: } 2[Cu(NH_3)_4]SO_4 + CO_2 + 3H_2O \rightleftharpoons Cu_2CO_3(OH)_2 + 4NH_3 + 2(NH_4)_2SO_4 \quad (2)$$

In a preliminary study, cyan precipitates indeed formed by bubbling CO_2 to an aqueous solution of **Complex 1** in the absence of ammonium carbamate. We then applied the method to recover Cu(II) from the catalytic urea formation described in entry 1 of Table 1. At the end of the reaction, ammonium carbamate and residual NH_3 were removed under vacuum at 50 °C. Upon bubbling the aqueous solution of the reaction mixture using CO_2, cyan precipitates formed. Without thoroughly removing NH_3, no precipitates formed, which is likely due to the high stability of $[Cu(NH_3)_4]^{2+}$ in the presence of NH_3.[26,27,38] The PXRD analysis suggests that this precipitate is amorphous. The FT-IR spectrum of this recovered material was virtually identical to that of the precipitates obtained from the preliminary study. The amorphous cyan precipitates have strong absorption for O−H (3286 cm^{-1}, broad) and carbonate C═O bonds (1058, 1382, and 1460 cm^{-1}, broad). These stretches resemble those of crystalline $Cu_2CO_3(OH)_2$: 3374 cm^{-1} for O−H and 1045, 1330, and 1409 cm^{-1} for C═O. The FT-IR spectra are available in Figure S5 of the Supporting Information. The cyan precipitates were filtered, dried, and recycled for catalytic urea synthesis, and water was removed from the filtered solution to obtain urea. Cu(II) was consistently recovered in a 66 ± 3% yield (triplicate) using this procedure. The lost Cu(II) was due to incomplete precipitation and the small, milligram scale of the experiment.

The recovered $Cu_2CO_3(OH)_2$ instantly dissolved in a 1 M ammonium carbamate solution (4 mM Cu). The UV−vis spectrum of this solution (λ_{max} = 630 nm) was similar to that of **Complex 1** in a 1 M ammonium carbamate solution (4 mM Cu). Under the reaction conditions described in entry 1 of Table 1, the recovered $Cu_2CO_3(OH)_2$ catalyzed urea formation in a 2% yield, which was less than that with **Complex 1** under otherwise identical reaction conditions (4% yield). Details of the catalyst recycling experiment are described in the Copper(II) Recovery by Precipitation with

https://doi.org/10.1021/acs.inorgchem.0c03467
Inorg. Chem. 2021, 60, 5573−5589

CO_2 and Catalytic Urea Formation by the Recovered Basic Copper Carbonate section.

Various reaction conditions were tested (Table 1). Compared to the conditions used in entry 1, increasing the volume of water from 0.5 mL (entry 1 in Table 1) to 5 mL (entry 3) led to no urea formation. Water is a side product of urea formation and can shift the equilibrium completely to the reactant side. Nevertheless, when the amount of water is lowered to 28.9 ± 3.2 μL (eq 2 in Scheme 3 and entry 4), a much higher urea yield of 18 ± 6% was obtained. Water serves as a solvent for **Complex 1**. We attempted to increase the reaction yield by minimizing the amount of CO_2 and NH_3 gases in the headspace of the reactor because the amount of ammonium carbamate could be lowered by the decomposition of ammonium carbamate to CO_2 and NH_3 (Scheme 1). In the reaction described in entry 5 in Table 1, the headspace of the reactor was minimized by filling the reactor with the reaction mixture. As a result, the scale of the reaction is increased 4-fold, but otherwise under the same temperature, reaction time, and catalyst loading as shown in entry 4 in Table 1. However, the yield decreased to 1.5% compared to the 18 ± 6% yield of entry 4.

No urea formed when lowering the temperature from 120 to 90 °C, presumably due to the low reaction rate (entry 6). The copper(II) sulfate pentahydrate complex is as active as **Complex 1** (entry 7 vs entry 1), possibly due to the in situ formation of $[Cu(NH_3)_4]^{2+}$ from copper(II) cations and ammonia.[28] The ammonia ligands likely originate from the decomposition of the ammonium carbamate (Scheme 1) present in the solution. Despite the similar effect in catalysis, the simple copper(II) sulfate salt is an unstable precatalyst that was avoided for this rigorous study on the mechanism of catalysis.

We lowered the catalyst loading from 1% (entry 1) to 0.2% (entry 8) to evaluate the maximum catalyst turnover, with the substrate in a 500-fold excess relative to the catalyst. A catalyst turnover of 40 and a urea yield in 8% were obtained after 15 h at 120 °C (entry 8). Under otherwise identical conditions, doubling the reaction time to 30 h lowered the yield to 4% (entry 9). The decrease in the urea yield over time is possibly due to the formation of byproducts, such as ammonium bicarbonate and cyanuric acid.[1,3,15]

In the absence of water, increasing the temperature from 120 to 150 °C reduced the reaction time from 15 to 1 h, and a 13% urea yield was obtained using a catalyst loading of 5% (entry 10). With only a 1% catalyst loading and at 150 °C, the yield dropped to 5% (entry 11). In the presence of CO_2 at 300 psi (measured at 150 °C), the yield of urea was increased only slightly from 5 to 8% (entry 12). Compared to entry 11, adding water (entries 13 and 14) did not improve the yield. We lowered the catalyst loading to 0.2% to evaluate the maximum catalyst turnover at 150 °C in the absence of water. Up to 75 turnovers and a 15% urea yield were obtained in 17 h (entries 15−17).

Control experiments in the absence of **Complex 1** showed that no significant (<1%) urea formed (entry 2 in Table 2) under otherwise identical conditions to entry 10 in Table 1. On its own, water did not catalyze urea formation at 150 °C (entry 3 in Table 2). With 28.9 ± 3.2 μL of water but without **Complex 1**, a much lower yield of urea was obtained (3% yield in entry 4 in Table 2) than the reaction with **Complex 1** (18 ± 6% yield in entry 4 in Table 1). Water is a side product in urea formation. Despite a previous report[7] that indicated the catalytic effect of water in urea formation, no significant urea formed under our conditions using water without **Complex 1**.

Comparison to Urea Formation Catalyzed by CuO. The slow urea formation, catalyzed by CuO and performed in the solid state, took 3 days (Scheme 2), and the rate could be limited by diffusion. We reproduced the results for the CuO-catalyzed urea formation from ammonium carbamate.[5] CuO catalyzed the formation of urea from ammonium carbamate at 120 °C and over 3 days (Scheme 2 and entry 1 in Table 3).

Table 3. Urea Formation from Ammonium Carbamate Catalyzed by CuO[a]

entry	catalyst	time	urea yield (%)
1	CuO	3 days	22
2	CuO	15 h	3
3	CuO	3 h	<1

[a]Reaction conditions: 1% CuO catalyst, under air, in a 22 mL Hastelloy high-pressure metal reactor, at 120 °C, without water, and with 2.0 g or 26 mmol of ammonium carbamate starting material; analyzed by quantitative $^1H\{^{13}C\}$ NMR spectroscopy.

However, we obtained a yield of 22% by $^1H\{^{13}C\}$ NMR analysis, instead of the 54% yield previously measured using the weight of the crude product. Without CuO, only a 6% yield was obtained after 3 days under otherwise identical conditions. We analyzed and quantified the urea using $^1H\{^{13}C\}$ NMR spectroscopy, in DMSO-d6, and in the presence of benzene as an internal standard. The details are described in the Experimental Procedure section.

Reaction times of 3 and 15 h, instead of 3 days, were selected to study the initial stage of the CuO-catalyzed reaction. No significant (<1%) urea formed after 3 h (entry 2 in Table 3), and urea at a 3% yield was obtained after 15 h (entry 3 in Table 3). The low yields obtained after a short reaction time confirmed that the formation of urea from ammonium carbamate is slow at 120 °C. Therefore, a long reaction time of 3 days is necessary when using CuO as a catalyst.

CuO could not be recovered at the end of the 15 h reaction described in entry 2 in Table 3. The product mixture was purified by drying under vacuum and methanol extraction (see the Experimental Procedure section for details regarding the purification by methanol extraction). The solid, which is insoluble in methanol, was analyzed by PXRD. No CuO reflections were detected (<2 mg CuO of the 20 mg CuO catalyst), which was consistent with the decomposition of the CuO catalyst over 15 h. A PDF card of 04-007-0518 was used for the phase indexing of CuO (tenorite).

In the control experiment, we verified that a purchased sample of CuO in 20 mg (1% catalyst loading or 0.26 mmol) was readily detected via PXRD analysis. To mimic the setup and purification of the catalytic reaction, we performed another control experiment. CuO in 20 mg was mixed thoroughly with ammonium carbamate in 2.0 g. The ammonium carbamate was then removed via methanol extraction (see the Experimental Procedure section for details on methanol extraction). CuO, a dark solid that was insoluble in methanol, was dried under vacuum for 1 h and analyzed via PXRD spectroscopy. The CuO phase was identified using a scan rate of 2° 2θ per minute and a range of 15−80° 2θ. The 14.5 mg recovered sample containing the CuO was then mixed thoroughly with an internal standard (Co_3O_4 powder in 10.5 mg) for quantitation

https://doi.org/10.1021/acs.inorgchem.0c03467
Inorg. Chem. 2021, 60, 5573−5589

(spinel Co_3O_4, PDF card: 01-078-5632). A quantitative PXRD phase analysis was conducted using the Rietveld method[43−46] on the entire 25.0 mg of the combined sample.[43] No refinement on the preferred orientation was necessary. A CuO-to-Co_3O_4 mole ratio of 0.759:0.241, corresponding to 0.518:0.482 by weight, was measured. The mole number of the CuO was calculated using the mole number of Co_3O_4, and the recovery yield of CuO in this control experiment was 55% by mole. Details of this PXRD analysis are described in the Supporting Information.

In comparison, the reaction using **Complex 1** as the catalyst (entry 4 in Table 1) gave a comparable yield of urea formation in much less time than using CuO (entry 1 in Table 3): 15 h vs 3 days. Additionally, 29% of **Complex 1** was recovered at the end of the reaction, in contrast to CuO. The possibility that CuO decomposed and released Cu(II) ions in situ cannot be excluded.

Catalysis Mechanisms via Quantum Chemistry Calculations. *Structure of Ammonium Carbamate.* In the current study, ammonium carbamate is the reactant. The geometry optimization of ammonium carbamate gave a complex of carbamic acid and NH_3 as the global minimum (B in Figure S10 in the Supporting Information) at the B3LYP/6-31G** + SMD-water level of theory. Another structure is ammonium carbamate (C in Figure S10), which is 4.2 kcal/mol higher in Gibbs energy than the hydrogen-bonding carbamic acid + NH_3. The calculations with the compound method CBS-QB3 + SMD-water reduce their energy difference to 1.1 kcal/mol. For the Cu(II)$(NH_3)_4$-coordinated complexes, the carbamic acid + NH_3 structure (D in Figure S10) is 1.4 kcal/mol lower than the ammonium carbamate structure (E in Figure S10). Although the carbamic acid structure is lower in energy in both cases, the small Gibbs energy differences render the structural preference inconclusive. The situation that the ionic compounds of NH_4^+ turned out to be complexes between neutral compounds and NH_3 in theoretical studies has been reported.[7,47] The Cu(II)$(NH_3)_4$-ammonium carbamate and its conjugate acid, Cu(II)$(NH_3)_4$-carbamic acid + NH_3, can equilibrate due to the small difference in energy. For geometric parameters, the COOH...NH_3 distances (1.6116 Å for B and 1.5124 Å for D) in the carbamic acid + NH_3 complexes and the COO...HNH_3^+ distances (1.4989 Å for C and 1.5021 Å for E) in the ammonium carbamate ones are much shorter than the corresponding atomic distances in normal hydrogen bonds: the N...H distances are 1.80 and 2.16 Å in NH_3...H_2O and NH_3...NH_3 complexes (F in Figure S10), respectively, at the same level of theory. In the solid state, the COO...HNH_3^+ distances of ammonium carbamate obtained from the X-ray crystal structure range from 1.77 to 2.19 Å,[48] which are consistent with normal hydrogen bonds. The calculated COO...HNH_3^+ distance (1.4989 Å) of ammonium carbamate in the solution state is at least 0.27 Å shorter than those found in the solid state. In addition, the net charges on the shared H are close to 1 (the ATP charges are 0.8−1.0 on the central H), indicating that the hydrogen bond in ammonium carbamate has obvious ionic characteristics with or without being coordinated with Cu(II). Overall, the in silico solution structures suggest that the structural distinction between ammonium carbamate and carbamic acid + NH_3 is less clear-cut in the solution state than in the solid state, which is possibly due to the strong hydrogen bond interaction (broadly defined as an n-to-σ^* bonding interaction[49]) in the solution state. Therefore, both carbamate and carbamic acid were investigated for the Cu(II)-catalyzed urea synthesis.

Ammonium carbamate is a stable structure in the solid state and has been characterized by X-ray crystallography,[48] and carbamic acid is believed to be a transient intermediate in the dissociation of ammonium carbamate.[50−52] A Cu(II) complex coordinated by organic amine and organic carbamate ligands has been synthesized and characterized by X-ray crystallography.[53] The spectroscopic evidence for the existence of unsubstituted carbamic acid is rare,[54] but a dibenzyl-substituted carbamic acid has been made at 10 °C and characterized by IR spectroscopy (ν_{as}(COO) = 1640 cm^{-1}) and X-ray crystallography.[50] Low-temperature IR studies[54] suggest that the hydrogen-bond-stabilized zwitterion form of carbamic acid, $NH_3^+-CO_2^-$ (ν_{as}(COO) = 1595 cm^{-1}), is formed from CO_2, NH_3, and H_2O. Organic carbamic acid and its zwitterion form can interconvert.[52] Carbamic acid is extremely difficult to detect[50,55] because it is unstable against deprotonation by NH_3 and decarboxylation. However, the conjugate acid of carbamic acid, mono-O-protonated carbamic acid, has been made by Olah et al. using superacid at −78 °C and characterized by ^1H, ^{13}C, and ^{15}N NMR spectroscopy.[56]

Most of our experiments were performed at 120 °C. Although elevated temperatures generally disfavor the formation of carbamic acid, the hydrogen-bonded ν(N−H) signal of $NCOO^-$...$HNRH_2^+$ (R = ethylene group in tetraethylenepentamine, TEPA) is found to persist at 120 °C in an IR study on an immobilized TEPA sorbent with CO_2 and water.[57] By the calculations at the level of the B3LYP/6-31G** + SMD-water level of theory, we found that carbamate anion has a lower complexation energy (by 4−10 kcal/mol) than carbamic acid to $[Cu(II)(NH_3)_4]^{2+}$, indicating that carbamate anion is a better ligand than carbamic acid to $[Cu(II)(NH_3)_4]^{2+}$. However, in the presence of an associated NH_3, Cu(II)$(NH_3)_4$-carbamic acid + NH_3 can have lower or at least comparable Gibbs free energy to Cu(II)$(NH_3)_4$-ammonium carbamate. In addition, as shown by a simple test of the C−O(Cu) bond breakage (see Figures S11 and S12 in Section 2.3 of the SI), we find that the proton transfer (Mulliken charges and spin density on the shifting H are, respectively, 0.3−0.4e and <0.001) to the carboxylate oxygen was necessary to lower the transition-state energy for converting ammonium carbamate to urea. Thus, the coordinated carbamic acid intermediate needs to be considered in the catalytic mechanism study.

In our theoretical studies, we first study catalytic pathways involving the transient intermediate of carbamic acid. Then, we study the catalysis mechanisms using the complexed ammonium carbamate as the starting point of the catalyzed reaction. Finally, we briefly investigate the pathway with a coordinated carbamate anion in the absence of NH_4^+.

Identifying the Effective Catalyst Structure of ***Complex 1****.* We compared the stability of a series of copper(II)−ammonia complexes with various coordination numbers and ligands at the B3LYP/6-31G** + SMD-water and M02x/6-311++G-(3df,2pd) − SMD-water levels of theory. The 4-coordinate $[Cu(NH_3)_4]^{2+}$ is the most stable. The relative Gibbs free energies and structures are shown in Table S1 and Figure S1 in the Supporting Information.

We studied the aqueous coordination chemistry[33] of six-coordinate complexes, which include $[Cu(NH_3)_6]^{2+}$, $[Cu(NH_3)_4(H_2O)_2]^{2+}$, $[Cu(NH_3)_4(OH_2)SO_4]$, and $[Cu(NH_3)_4SO_4]$-ammonium carbamate (Figure S1 in the

https://doi.org/10.1021/acs.inorgchem.0c03467
Inorg. Chem. 2021, 60, 5573−5589

Supporting Information). Each complex has three coordination spheres: (1) the inner sphere, which consists of the $[Cu(NH_3)_4]^{2+}$ moiety with metal-to-ligand distances at ∼2.0 Å, (2) the middle sphere, which consists of ligands at a distance of ∼2.3 Å from the metal, and the outer sphere, which consists of ligands at a distance greater than 3.0 Å from the metal. The inner sphere, with four tightly bound NH_3 ligands, has a roughly square-planar geometry, while the inner and middle spheres together adopt a square-pyramidal geometry. The presence of a middle sphere is due to the Jahn−Teller distortion in d9 Cu(II). Finally, all three spheres fit into a loosely octahedral geometry. The molecule in the outer sphere can easily move away from its octahedral site to form hydrogen bonds with other ligands. For example, one H_2O in $[Cu(NH_3)_4(H_2O)_2]^{2+}$ is 3.46 Å from Cu(II), but the overall geometry is still octahedral (Figure S1). However, the geometry of $[Cu(NH_3)_6]^{2+}$ confirms another situation; the sixth NH_3 molecule moves away from the octahedral site and forms hydrogen bonds with one NH_3 molecule in the inner sphere. This unsymmetrical structure is 7.9 kcal/mol lower in total energy than the highly symmetrical octahedral structure at the B3LYP/6-31G** + SMD-water level (Table S1 and Figure S1). Our results are consistent with the study of water in the primary versus secondary coordination sphere in the copper(II)−ammonia system.[33,58] Pavelka et al. found that the 4-coordinate $\{[Cu(NH_3)_4]\cdot 2H_2O\}^{2+}$ complex, where two water molecules are hydrogen-bonded to NH_3 rather than coordinated to Cu(II), was more stable than the 6-coordinate $[Cu(NH_3)_4(OH_2)_2]^{2+}$ by 7.8 kcal/mol at the B3LYP/6-311++G(2df,2pd) level.[58] A decomposition analysis suggested that the stability of $\{[Cu(NH_3)_4]\cdot 2H_2O\}^{2+}$ was due to the higher covalency in the Cu−N bonds of $\{[Cu(NH_3)_4]\cdot 2H_2O\}^{2+}$ than that in $[Cu(NH_3)_4(OH_2)_2]^{2+}$. Overall, our calculations for $[Cu(NH_3)_4(H_2O)_2]^{2+}$ indicate that four NH_3 molecules are in the inner sphere, one H_2O molecule is in the middle sphere, and the other H_2O is in the outer sphere (Figure S1).

Our calculated solution structure of $[Cu(NH_3)_4(H_2O)_2]^{2+}$ agrees well with the solid-state X-ray structure of **Complex 1** ($[Cu(NH_3)_4(OH_2)]SO_4$). In the solid state, the single-crystal X-ray structure of **Complex 1** has a 5-coordinate, square-pyramidal geometry,[59] with the aqua ligand attached to the axial position via an elongated bond.[59] The water molecule bridges two Cu(II) at unequal distances to form a Cu−OH_2−Cu chain in the lattice. The X-ray structure was assigned as 5-coordinate and square-pyramidal due to the very long Cu...O distance (3.475 Å) for one of the two water molecules neighboring Cu(II). Remarkably, the calculated Cu−O bond lengths of $[Cu(NH_3)_4(OH_2)_2]^{2+}$ at 2.35 and 3.46 Å are >99.5% identical to those found in the single-crystal X-ray structure of **Complex 1** at 2.339 and 3.475 Å, respectively.[59] Following this convention, the calculated solution structure of $[Cu(NH_3)_4(OH_2)_2]^{2+}$ should also be described as 5-coordinate and square-pyramidal. One of the two water molecules should thus be considered as a solvate rather than a ligand.

The fact that three coordination spheres exist in Cu(II) complexes also sheds light on the ambiguous solution structure of Cu(II) complexes in the literature. The precise aqueous solution structure regarding the number of aqua ligands in copper(II)−ammonia complexes remains inconclusive.[27] The formulas $[Cu(NH_3)_4]^{2+}$ and $[Cu(NH_3)_4(OH_2)_2]^{2+}$ are used interchangeably in the literature.[26−28,34,60,61] A coordination number of 6 for $[Cu(NH_3)_4(OH_2)_2]^{2+}$ was assigned by Bjerrum et al. in the 1950s based on the presumed tetragonal bipyramidal structure.[26,27] In the 1970s, Hathaway et al. argued against the existence of a 4-coordinate square-planar tetraamminecopper(II) complex due to the lack of conclusive evidence in solid-state studies. Since there are three coordination spheres, copper(II)−ammonia complexes could be detected as having the characteristics of different coordination numbers, depending on the conditions and detection methods.

Based on its stability in water, the 4-coordinate $[Cu(NH_3)_4]^{2+}$ complex is likely an effective catalyst structure for the urea formation in Scheme 3. The data in Table S1 show that $[Cu(NH_3)_4]^{2+}$ is more stable than $[Cu(NH_3)_4(OH_2)_2]^{2+}$ by 10.3−14.8 kcal/mol. The Gibbs free energies for copper(II)−ammonia complexes relative to Cu(II) ions have large negative values (column I in Table S1 of the Supporting Information). However, the relative Gibbs free energies become positive if the reference is $[Cu(NH_3)_4]^{2+}$ (column II in Table S1). Based on the experimental speciation diagram of the copper(II)−ammonia system,[27,28,38,60] $[Cu(NH_3)_4]^{2+}$ is the major species (60−90%) at an ammonia concentration of 0.01−1 M at room temperature. At an ammonia concentration of 0.5−10 M, $[Cu(NH_3)_4]^{2+}$ and $[Cu(NH_3)_5]^{2+}$ coexist.[27] $[Cu(NH_3)_4]^{2+}$ can exist as the major species at a temperature range from 30 to 150 °C at a neutral or basic pH.[38] In contrast, the formation of $[Cu(NH_3)_3]^{2+}$ or $[Cu(NH_3)_5]^{2+}$ is less favorable than that of $[Cu(NH_3)_4]^{2+}$. As summarized in the equations below, the $[Cu(NH_3)_4]^{2+}$ complex has the highest overall formation constant,[26−29,31] $\beta_4 = K_1K_2K_3K_4 = 0.992-2.08 \times 10^{13}$. The successive formation constant of $[Cu(NH_3)_4]^{2+}$ is favorable, $K_4 = 120$, and the formation of $[Cu(NH_3)_5]^{2+}$ is unfavorable, $K_5 = 0.3$. The $[Cu(NH_3)_6]^{2+}$ complex could only be made in liquid ammonia ($K_6 = 0.003$)[29,30] and is unlikely to form under our conditions. Although we could not rule out the possibility that the minor species $[Cu(NH_3)_3]^{2+}$ or $[Cu(NH_3)_5]^{2+}$ are involved in catalysis, they are in rapid equilibrium with $[Cu(NH_3)_4]^{2+}$. Cu(II) has a d9 electron configuration and is kinetically labile.[62]

$$[\mathbf{Cu(NH_3)_3}]^{2+} + \mathbf{NH_3} \rightleftharpoons [\mathbf{Cu(NH_3)_4}]^{2+} \quad \mathbf{K_4} = 120$$

$$\boldsymbol{\beta_4} = 0.992 - 2.08 \times 10^{13}$$

$$[Cu(NH_3)_2]^{2+} + NH_3 \rightleftharpoons [Cu(NH_3)_3]^{2+} \quad K_3 = 800$$

$$\beta_3 = 2.88 \times 10^{10}$$

$$[Cu(NH_3)_4]^{2+} + NH_3 \rightleftharpoons [Cu(NH_3)_5]^{2+} \quad K_5 = 0.3$$

$$\beta_5 = 8.64 \times 10^{9}$$

$$[Cu(NH_3)_5]^{2+} + NH_3 \rightleftharpoons [Cu(NH_3)_6]^{2+} \; K_6 = 0.003$$

$$\beta_6 = 2.59 \times 10^{7}$$

Our experimental results also support the presence of $[Cu(NH_3)_4]^{2+}$. When **Complex 1** was dissolved in water or in a 1 M aqueous ammonia solution, the UV−vis absorption at λ_{max} = 605 nm was consistent with the literature values[26,38] of $[Cu(NH_3)_4]^{2+}$ at λ_{max} = 590−598 nm. The 7−15 nm red shift is due to the overlap[27,38] with minor species that are at equilibrium with $[Cu(NH_3)_4]^{2+}$; the minor species is $[Cu(NH_3)_3]^{2+}$ (λ_{max} = 621−655 nm) when measured in water or $[Cu(NH_3)_5]^{2+}$ (λ_{max} = 640 nm) when measured in 1 M

https://doi.org/10.1021/acs.inorgchem.0c03467
Inorg. Chem. 2021, 60, 5573−5589

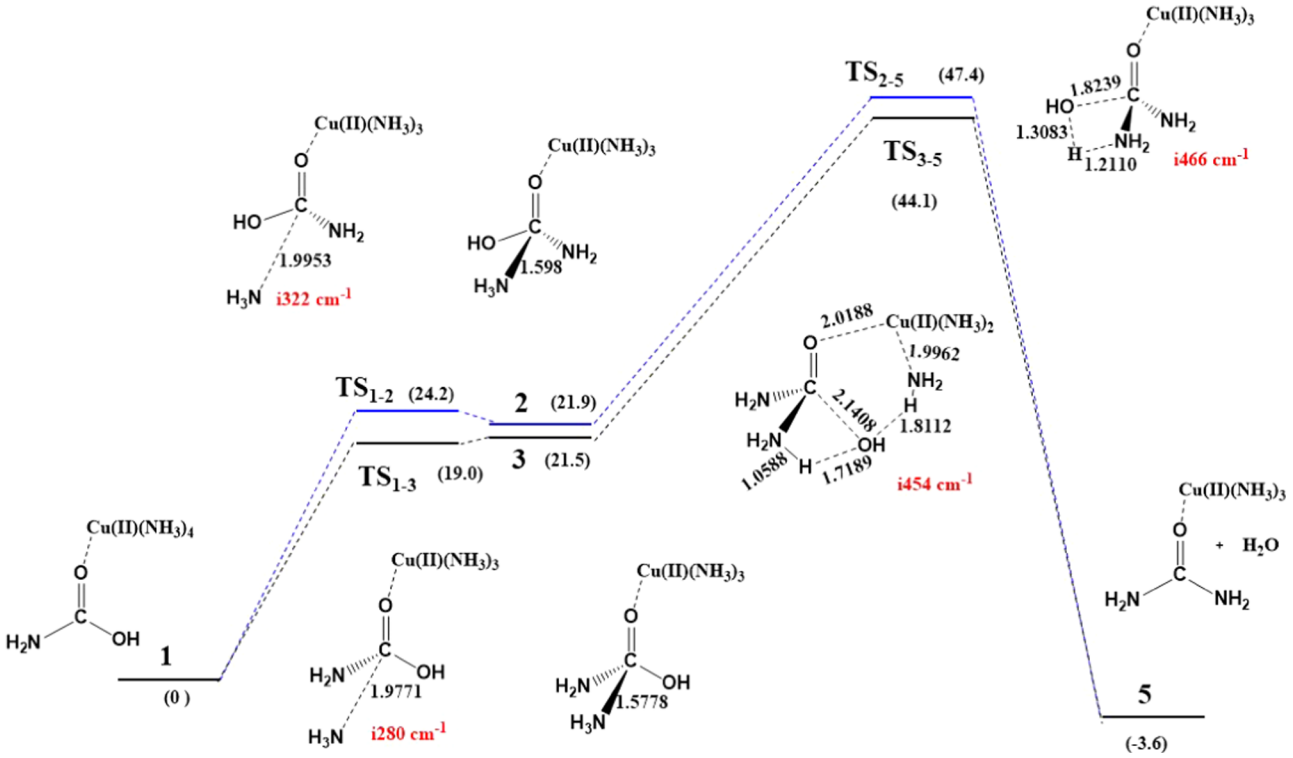

Figure 1. Two pathways are identified for the mechanism in Scheme 4, going from the copper(II)−carbamic acid intermediate **1** to the copper(II)−urea intermediate **5**. Top (blue): the pathway goes through adduct intermediate **2** and the corresponding $\mathbf{TS}_{1-2}$ and $\mathbf{TS}_{2-5}$. Bottom (black): the pathway goes through adduct intermediate **3** and the corresponding $\mathbf{TS}_{1-3}$ and $\mathbf{TS}_{3-5}$. There is a hydrogen bond between the OH group and an NH_3 ligand in $\mathbf{TS}_{3-5}$. All of the intermediates have a 2+ charge. The numbers in the brackets are relative Gibbs free energies in kcal/mol. Bond lengths are in Å, and the red numbers are imaginary frequencies in cm^{-1}.

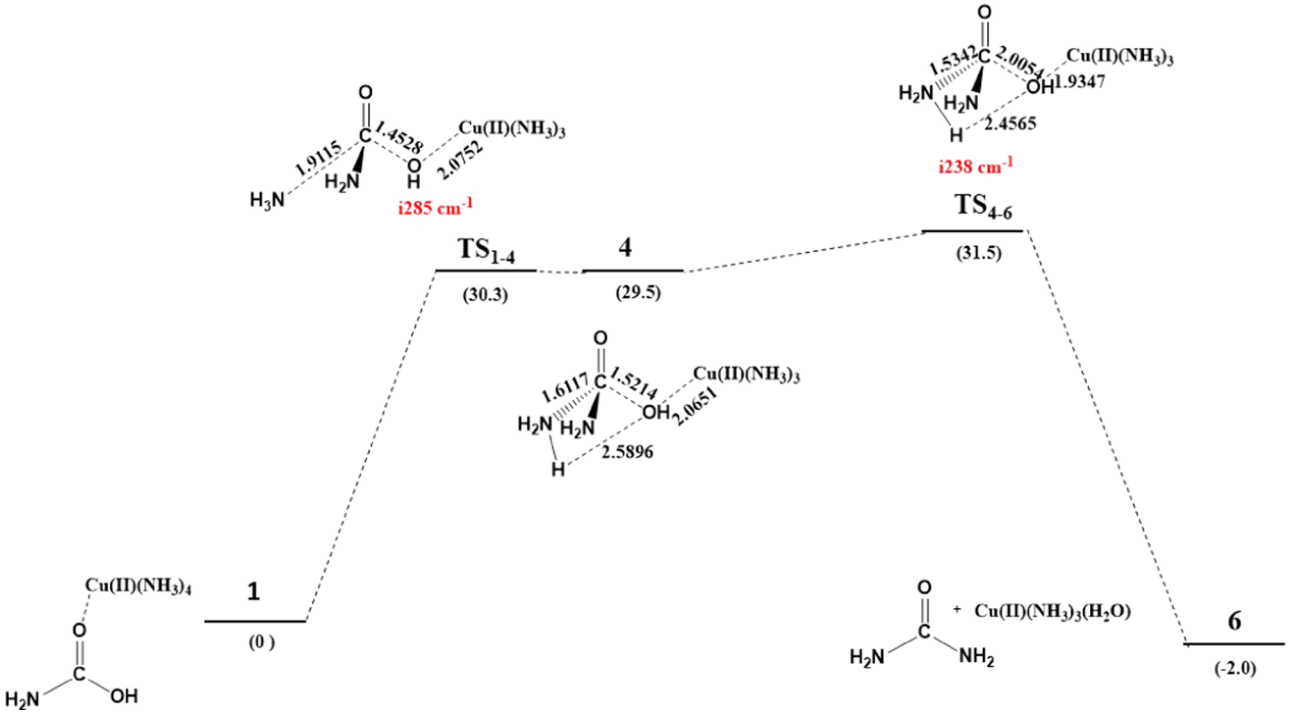

Figure 2. Alternative pathway is identified for the mechanism in Scheme 4. Intermediate **1** transforms into the adduct intermediate **4**, in which $[Cu(NH_3)_3]^{2+}$ coordinates with the leaving OH group. Then, Cu(II) facilitates the removal of the OH group to form H_2O via $\mathbf{TS}_{4-6}$. The numbers in the parentheses are relative Gibbs free energies in kcal/mol. The bond lengths are in Å, and red numbers are imaginary frequencies in cm^{-1}. The overall barrier is 31.5 kcal/mol. This pathway is the most favorable for the urea formation catalyzed by **Complex 1**.

https://doi.org/10.1021/acs.inorgchem.0c03467
Inorg. Chem. 2021, 60, 5573−5589

Scheme 4. Proposed Reaction Pathway[a]

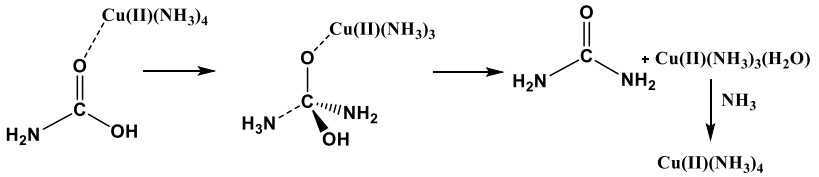

[a]Complex between $[Cu(NH_3)_4]^{2+}$ and carbamic acid gives rise to an adduct intermediate to activate NH_3 and then the adduct intermediate internally transfers a proton and eliminates H_2O, producing urea. The free NH_3 from ammonium carbamate (in equilibrium with carbamic acid and NH_3) regenerates the $[Cu(NH_3)_4]^{2+}$ catalyst.

NH_3.[26,38] The molar absorptivity of 53.6 L mol^{-1} cm^{-1} is also consistent with $[Cu(NH_3)_4]^{2+}$ at 49.8−55 L mol^{-1} cm^{-1}.[38] The results from the UV−vis analysis are consistent with the speciation diagram of the copper(II)−ammonia system,[27,28,38,60] where the major copper(II) species (60−90%) in water is $[Cu(NH_3)_4]^{2+}$ at an ammonia concentration of 0.01−1 M.[27] Details of the UV−vis analysis are described in the Experimental Procedure section.

Catalytic Pathways Involving a Carbamic Acid Intermediate. Mechanisms That Involve Adduct Intermediates. The stability of the 4-coordinate $[Cu(NH_3)_4]^{2+}$ complex suggested that 4-coordinate Cu(II) intermediates, with the general formula of $[Cu(NH_3)_3L]^{2+}$ (L = a neutral ligand), could also be stable. Therefore, we focused on 4-coordinate Cu(II) intermediates when investigating the mechanisms (Figures 1 and 2). The transition states with the 5-coordinate Cu(II) were difficult to locate. We located two transition states with the 5-coordinate Cu(II) (Figure S3), in which the carbamic acid ligand was weakly associated with Cu(II) in the middle and outer coordination spheres. In contrast, the transition states with the 4-coordinate Cu(II) were readily located. The carbamic acid ligand in the 4-coordinate Cu(II) intermediates was consistently located in the inner coordination sphere of Cu(II), occupying one site of the square-planar structure. This structure allows Cu(II) to exert a maximum influence on the carbamic acid ligand.

The proposed reaction pathway is shown in Scheme 4. The reaction starts with a complex between the carbamic acid and $[Cu(NH_3)_4]^{2+}$, as shown in intermediate **1** in Figure 1. Intermediate **1** is 10.2 kcal/mol uphill from $[Cu(NH_3)_4]^{2+}$ and carbamic acid, separately (Table S1 in the Supporting Information). An NH_3 ligand then performs a nucleophilic attack on the carbonyl group of the carbamic acid, giving rise to an adduct intermediate. Meanwhile, the sp^2 carbon of carbamic acid becomes sp^3. The incoming NH_3 in the adduct intermediate is activated to lose a proton. Then, the proton is transferred from the incoming NH_3 to the OH group. As a result, water is eliminated, and urea is formed. A free NH_3 molecule from the reaction mixture regenerates the $[Cu(NH_3)_4]^{2+}$ catalyst from $[Cu(NH_3)_3(H_2O)]^{2+}$ and completes the catalytic cycle. The source of NH_3 is ammonium carbamate, as discussed in the Structure of Ammonium Carbamate section.

Indeed, we located the adduct intermediates **2** and **3** at the B3LYP/6-31G** + SMD-water level of the theory (Figure 1). These intermediates have long C...NH_3 distances at 1.598 and 1.5778 Å, respectively, and the carbon adopts a tetrahedral geometry (Figure 1). Intermediates **2** and **3** can easily reverse to **1** through transition states $\mathbf{TS_{1-2}}$ and $\mathbf{TS_{1-3}}$. The NH_3 is stretched much further away from carbon in the transition states, where the C...NH_3 distances are 1.9953 Å for **2** and 1.9771 Å for **3**. The backward activation barrier is small (2.3 kcal/mol) for **2** and negative for **3** (−2.5 kcal/mol). The negative barrier is due to the unfavorable zero-point vibrational energy (ZPVE) and unfavorable entropy for **3**. Thus, **2** and **3** are shallow minima on the potential energy surface. Then, **2** and **3** internally transfer protons and remove the OH groups through $\mathbf{TS_{2-5}}$ and $\mathbf{TS_{3-5}}$ to form a copper(II)−urea complex **5**. The activation barriers, in Gibbs free energies, are 25.5 and 22.6 kcal/mol for **2** and **3**, respectively. The two pathways are very similar, except that the OH group in **2** is trans- to Cu(II), while that of **3** is cis- to Cu(II). The cis- configuration in **3** allows its OH group to form a hydrogen bond with an NH_3 ligand in $\mathbf{TS_{3-5}}$. Finally, the catalyst $[Cu(NH_3)_4]^{2+}$ is regenerated in the presence of NH_3 to complete the catalytic cycle. This step is omitted in Figure 1. The formation of intermediate **2** reduces a potentially high barrier (47.4 kcal/mol at 298.15 K, 48.0 kcal/mol at 393.15 K) into two smaller barriers (24.2 and 25.5 kcal/mol at 298.15 K; 24.9 and 25.4 kcal/mol at 393.15 K). Intermediate **3** might not play a significant role due to the negative barrier to convert back to **1**. The relative values at 120 °C (393.15 K) are estimated using the equation $\Delta G^0 = \Delta H^0 - T\Delta S^0$. The Gibbs energy differences between the two temperatures are generally less than 1 kcal/mol (Table S2).

In the alternative reaction pathway shown in Figure 2, the carbamic acid intermediate **1** transforms into the adduct intermediate **4**, which is a linkage isomer of **2** and **3**. For **4**, Cu(II) coordinates with the OH group of carbamic acid, whereas for **2** and **3**, Cu(II) coordinates with the carbonyl group. Intermediate **4** is 7.6 kcal/mol higher in Gibbs free energy than **2** because the Cu(II)...OH π-donor interaction in **4** is less favorable than the Cu(II)...O=C π-acceptor interaction in **2**. However, the activation barrier following **4**, $\mathbf{TS_{4-6}}$, is merely 2.0 kcal/mol, whereas the activation barrier following **2**, $\mathbf{TS_{2-5}}$, is much higher, at 25.5 kcal/mol. This inverse relationship between the ground-state energy of an intermediate and its activation barrier is a well-documented phenomenon in transition-metal catalysis.[63,64] Namely, a high-energy intermediate can lead to a lower activation barrier than a stable intermediate can. In $\mathbf{TS_{4-6}}$, the coordination of $[Cu(NH_3)_3]^{2+}$ to the OH group apparently makes the OH a better leaving group. The elimination of an OH group or breaking a C−O bond is a great challenge in organic synthesis.[65] Leaving-group activation is an effective strategy for breaking C−O bonds, as seen in the recent reports of the organocatalytic Mitsunobu reaction[66] and the mercury(II)-catalyzed C−O bond breakage.[67] In the final step of the reaction, the catalyst $[Cu(NH_3)_4]^{2+}$ is regenerated in the presence of NH_3 to complete the catalytic cycle. This step is omitted in Figure 2. This pathway has a rate-limiting step with an activation barrier of 30.3 kcal/mol at 298.15 K (30.9 kcal/

https://doi.org/10.1021/acs.inorgchem.0c03467
Inorg. Chem. 2021, 60, 5573−5589

mol at 393.15 K; Table S2). Again, the formation of intermediate 4 is important to reduce activation energies.

Other Possible Pathways. Three possible pathways were investigated in an early computational study[7] for urea formation in the gas phase and in the absence of a metal catalyst. The study was conducted at the B3LYP/6-31G** level of theory and without a continuum solvent model. These pathways are shown below. The respective activation barriers for the two steps in mechanism (a) are 51.5 and 38.7 kcal/mol, and 60.4 and 27.9 kcal/mol in mechanism (b). In mechanism (c), the activation barrier is 56.0 kcal/mol (these values are the Gibbs free energy).

(a) Elimination−addition mechanism

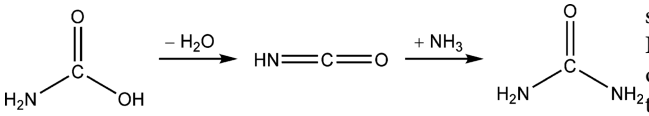

(b) Addition−elimination mechanism

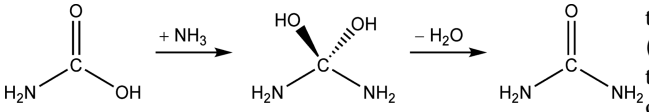

(c) Concerted mechanism

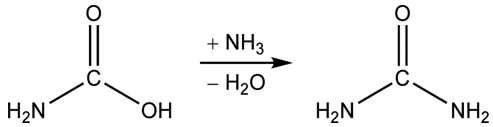

Since the elimination−addition mechanism (a) is the most kinetically favorable, we explored the effect of a $[Cu(NH_3)_4]^{2+}$ catalyst using this mechanism. The pathway involves two steps: (1) the elimination of water to form isocyanic acid and (2) the addition of ammonia to isocyanic acid to form urea. Specifically, we examined how using a continuum solvent model could change the activation barriers and whether $[Cu(NH_3)_4]^{2+}$ could catalyze the urea formation via mechanism (a).

The reported[7] intermediates and transition states for mechanism (a) were reoptimized at the B3LYP/6-31G** + SMD-water level. The solvent effect increases the activation barrier in the first step from 51.5 to 53.5 kcal/mol and reduces that in the second step from 38.7 to 26.2 kcal/mol. We then tested the two-step mechanism (a) in the presence of the $[Cu(NH_3)_4]^{2+}$ catalyst at the B3LYP/6-31G** + SMD-water level. In this pathway, a carbamic acid replaces an NH_3 ligand in $[Cu(NH_3)_4]^{2+}$ to give $[Cu(NH_3)_3(L)]^{2+}$ (L = carbamic acid) and NH_3. The Cu(II) can either coordinate with the NH_2 group (N-coordination) or the carbonyl oxygen (O-coordination) of carbamic acid. Both cases were investigated. The $[Cu(NH_3)_3(L)]^{2+}$ intermediate then undergoes step 1 to form a copper(II)-bound isocyanic acid intermediate upon the loss of H_2O, followed by step 2 to form a copper(II)-bound urea upon the nucleophilic addition of NH_3 to the copper(II)-bound isocyanic acid (Figure S2 in the Supporting Information). Four-coordinate Cu(II) intermediates were studied throughout. The two barriers for steps 1 and 2 of mechanism (a) are 62.5 and 37.6 kcal/mol for the N-coordination or 56.3 and 32.7 kcal/mol (O-coordination), respectively. The details are described in Figure S2 in the Supporting Information. The presence of $Cu(II)(NH_3)_4$ increases the barrier of step 1 in mechanism (a). Thus, it is unlikely for $Cu(II)(NH_3)_4$ to catalyze urea formation through mechanism (a).

In line with the work by Tsipis et al.,[7] we also performed extensive studies on mechanism (a) in the presence of $Cu(II)(NH_3)_4$ at the B3LYP/6-31G** level of theory, i.e., first isocyanic acid was produced (step 1) and then urea was produced through the elimination of H_2O. Many detailed steps were considered in the reaction mechanisms. Since the overall number of molecules was not the same for all of the considered steps in these studies, the relative energies were compared for the same elementary steps to gain useful information. The results are summarized in the Supporting Information. The solvent effects are not included in the calculations in the Supporting Information. It was clear that H_2O could significantly reduce the reaction barriers in the investigated H-transfer/H-extraction elementary reactions. In the formation of isocyanic acid (Figure S6), the involvement of H_2O reduced the reaction barriers from 52.2 to 29.1 kcal/mol. In addition, in the formation of urea (N-coordination; Figure S8), the involvement of H_2O reduced the reaction barriers from 26.6 to 15.5 kcal/mol. Finally, in another formation of urea reaction (O-coordination; Figure S9), the involvement of H_2O reduced the barrier from 18.7 to 4.5 kcal/mol. However, the formation of isocyanic acid reaction (Figure S6) still had a substantial overall barrier (37.0 kcal/mol).

We were also interested in the role of NH_3 as a cocatalyst because NH_3 would be around when ammonium carbamate converted to carbamic acid and NH_3. In the formation of isocyanic acid (Figure S7 in the Supporting Information), a series of intermediates and transition states were located. It seemed that a large barrier was separated into several smaller barriers, so the reaction activation barriers were significantly reduced. When we investigated the structural details of the intermediates and transition states, we noticed that there were large structural variations with small energy differences, so that solvent effects should be considered for reliable conclusions. In the formation of urea (N-coordination; Figure S8), the involvement of NH_3 showed a TS with NH_4^+ moiety and the barrier (27.9 kcal/mol) was virtually the same as the noninvolvement of NH_3 (26.6 kcal/mol). In another formation of urea reaction (O-coordinate; Figure S9), no transition states could be located. To draw a reliable conclusion, we included solvent effects with a continuous PCM model (SMD-water) to reinvestigate the role of NH_3 in the formation of isocyanic acid (Figure S3 in the Supporting Information). The transition state was found to have one NH_4^+ unit (the Mulliken charge for the NH_4 unit was +0.925, and the APT charge was +1.06), while the net charge on N(H) was −0.729 (Mulliken) or −1.135 (APT). The activation barrier was 19.3 kcal/mol, but detailed intrinsic reaction coordinate (IRC) analyses indicated that both forward and reverse reaction paths lead to the same initial complex structure.

Discussions on the Role of Cu(II). Cu(II) is a borderline Lewis acid.[68] Therefore, it coordinates favorably with the oxygen atoms of carbamic acid. Cu(II) can coordinate with carbonyl oxygen, rendering it more susceptible to nucleophilic attack by NH_3 (Scheme 4 and Figures 1 and 2). Upon a nucleophilic attack, an adduct intermediate bearing a tetrahedral carbon is formed (Scheme 4). Alternatively, Cu(II) can coordinate with the OH group on the tetrahedral carbon and facilitate the elimination of H_2O (Figure 2). The activation of the OH leaving group of a tetrahedral carbon intermediate could be the key to catalyze urea formation. Without the

https://doi.org/10.1021/acs.inorgchem.0c03467
Inorg. Chem. 2021, 60, 5573−5589

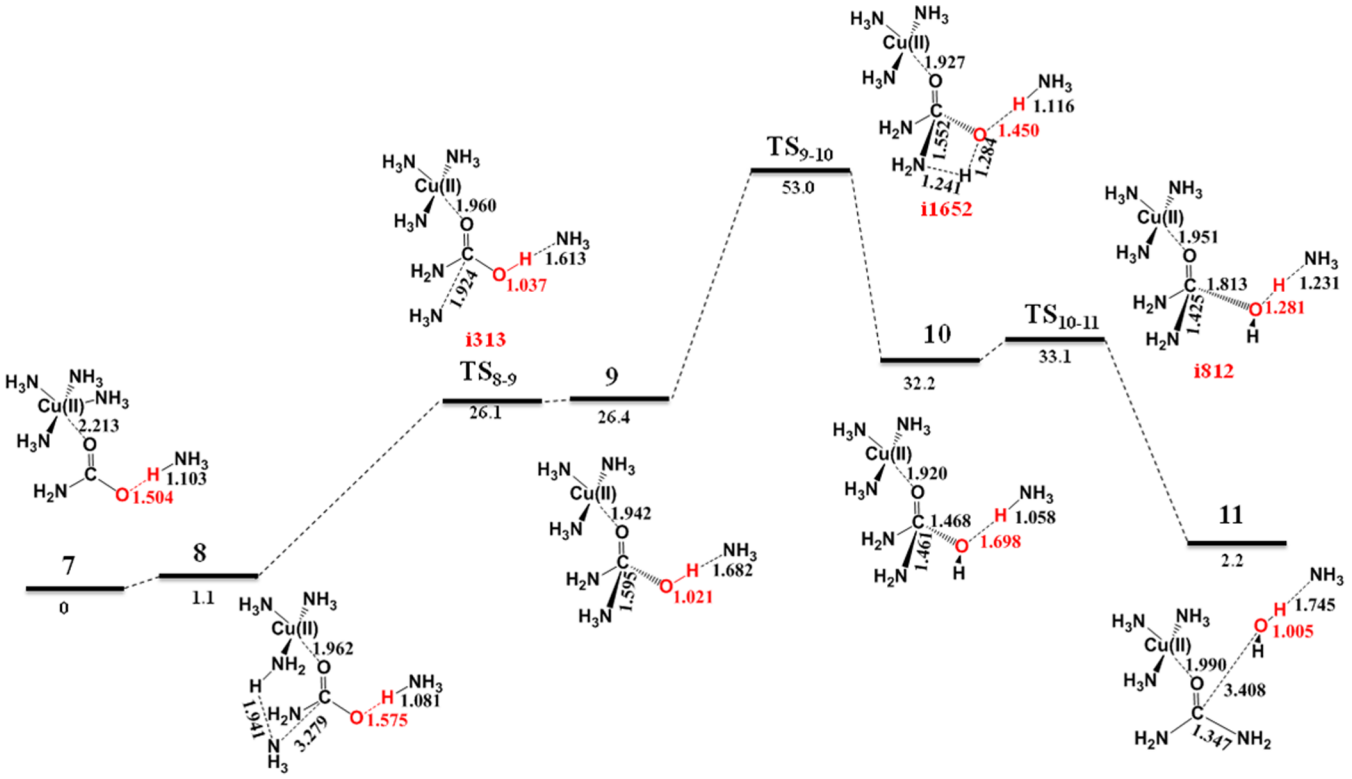

Figure 3. Pathway with ammonium carbamate is identified based on a similar mechanism shown in Scheme 4. The 5-coordinate Cu(II)−complex **7** rearranges to 4-coordinate Cu(II)−complex **8**, which then forms adduct intermediate **9** through $\mathbf{TS}_{8-9}$. An internal H-transfer forms another adduct intermediate **10** through $\mathbf{TS}_{9-10}$. Finally, the NH_4^+ facilitates the removal of H_2O to produce the formation of urea. The numbers in the parentheses are relative Gibbs free energies in kcal/mol. The bond lengths are in Å, and red numbers are imaginary frequencies in cm^{-1}.

formation of an adduct intermediate with a tetrahedral carbon, the activation barriers for urea formation are high, as discussed in the Other Possible Pathways section. The proposed mechanism in the Mechanisms That Involve Adduct Intermediates section can be considered as a combination of mechanisms (b) and (c), which are discussed in the Other Possible Pathways section.

Cu(II) is also a late-transition metal with a partially filled $3d^9 4s^0$ electron configuration. Therefore, its high effective nuclear charge and significant crystal-field stabilization energy[61,62] enable the formation of stable 4-coordinate, square-planar complexes. Although 4-coordinate, square-planar structures are mostly found in d8 metals, such as Ni(II), Pd(II), Ir(I), and Pt(II),[61,62] our calculations suggested that the 4-coordinate $[Cu(NH_3)_4]^{2+}$ is more stable in water than the 6-coordinate $[Cu(NH_3)_4(H_2O)_2]^{2+}$ is. This preference for a coordination number of 4 can be understood using the three coordination spheres discussed in the Structure of Ammonium Carbamate section.

Cu(II) has a strong tendency to form the 4-coordinate $[Cu(NH_3)_4]^{2+}$ complex, so that the reaction mixtures are in favor of $[Cu(NH_3)_4]^{2+}$, CO_2, and $2NH_3$. Intermediate **1** is 8.1 kcal/mol higher (14.6 kcal/mol at 393.15 K; Table S2) in Gibbs energy than $[Cu(NH_3)_4]^{2+}$, CO_2, and NH_3, i.e., the equilibrium constant K toward **1** is only 1.15×10^{-6} at 298.15 K (7.65×10^{-9} at 393.15 K, using $K = e^{-\Delta G/RT}$); however, the carbamic acid and the corresponding Cu(II) adduct intermediates (e.g., **2** and **4**) are necessary to synthesize urea. The relatively high barriers (>25 kcal/mol) could be consistent with a slow and endothermic reaction in experiments. For the rational design of transitional metal catalysts for urea synthesis, our study suggests that active catalysts can be screened computationally for low barriers in the proton transfer and C−O bond breakage steps that are described in Figures 1 and 2. In addition, the catalyst should be stable in the presence of NH_3 or it could be converted to a metal−ammonia complex in situ, such as the case for $[Cu(OH_2)_5]SO_4$ vs **Complex 1** that is described in entry 7 in Table 1.

Catalytic Pathways Involving Complexed Ammonium Carbamate and Complexed Carbamate in the Absence of NH_4^+. Figure 3 shows the catalytic mechanism using the complex of ammonium carbamate and $Cu(II)(NH_3)_4$ as the starting point. In step 1, the 5-coordinate Cu(II)−complex **7** rearranges to the 4-coordinate Cu(II)−complex **8** by moving away one coordinate NH_3 ligand so that the ammonium carbamate ligand moves from the middle coordination sphere to the inner coordination sphere (the Cu...O distance shortens from 2.213 to 1.962 Å). In complex **8**, the reacting NH_3 ligand forms a hydrogen bond with one of the remaining NH_3 molecules on Cu(II) (the N...H distance is 1.941 Å) and positions toward the central carbon of ammonium carbamate (the N...C distance is 3.279 Å). The total Gibbs energy slightly increases in the rearrangement (1.1 kcal/mol). In step 2, the reacting NH_3 molecule in complex **8** attacks the central C with its lone pair to form adduct intermediate **9** through transition-state $\mathbf{TS}_{8-9}$ (the reaction barrier is 26.1 kcal/mol). The adduct complex **9** is significantly different from $\mathbf{TS}_{8-9}$ in the N...C distances (1.595 vs 1.924 Å), but it is slightly higher than $\mathbf{TS}_{8-9}$ in the total Gibbs energy due to the contributions from entropy and zero-point vibrational energy (ZPVE). In step 3, an internal H-transfer converts complex **9** to complex **10** through $\mathbf{TS}_{9-10}$. It is interesting that any complexes similar to

https://doi.org/10.1021/acs.inorgchem.0c03467
Inorg. Chem. 2021, 60, 5573−5589

10 are not located in pathways involving carbamic acid (Figures 1 and 2). Finally, the removal of a H_2O molecule through $\mathbf{TS_{10-11}}$ produces urea with a small activation energy (0.9 kcal/mol). Here, the activation barriers of the elementary steps are relatively higher than those of the corresponding steps with carbamic acid: 26.1 kcal/mol ($\mathbf{TS_{8-9}}$) vs 24.2/19.1 kcal/mol ($\mathbf{TS_{1-2}}$/$\mathbf{TS_{1-3}}$) and 26.6 kcal/mol ($\mathbf{TS_{9-10}}$) vs 25.5/22.6 kcal/mol ($\mathbf{TS_{2-5}}$/$\mathbf{TS_{3-5}}$). Intermediate **7** is 2.9 kcal/mol higher in Gibbs energy than $Cu(II)(NH_3)_4 + CO_2 + 2NH_3$ at the B3LYP/6-31G** + SMD-water level of theory (Table S2).

It is interesting that the COO...H...NH_3 unit of ammonium carbamate is more like COO−H...NH_3 only in $\mathbf{TS_{8-9}}$ and complex **9**, possibly because complex **9** and $\mathbf{TS_{8-9}}$ have zwitterion characteristics. From **8** to **9**, the reacting NH_3 molecule loses electrons (ATP charges from +0.026 to +0.169) and the H in the hydrogen bond (in red color in Figure 3) gains electrons (ATP charges from +0.750 to +0.743). The presence of NH_4^+ enables the formation of intermediate **9** that has carbamic acid characteristics, so that the overall reaction barrier of 53.0 kcal/mol uphill from intermediate **7** reduces to two medium barriers (24.9 and 26.9 kcal/mol at 393.15 K; Table S2).

Since Cu(II) possibly forms a complex with a carbamate anion,[53,55,69] the reaction pathway involving $[Cu(NH_3)_4]^{2+}$ and a coordinated carbamate anion, in the absence of the NH_4^+ ion from ammonium carbamate, was searched at the B3LYP/6-31G** + SMD-water level of theory. Figure S13 is focused on the intermediates and transition states involved in the key step of the C−O bond breakage. The 5-coordinate Cu(II)−complex **12′** rearranges to a more stable (by 2.95 kcal/mol) 4-coordinate complex **12**, in which the reacting NH_3 molecule forms hydrogen bonds with a carbamate anion (2.3103 Å) and an NH_3 ligand of Cu(II) (1.930 Å). A shallow adduct intermediate similar to **9** in Figure 3 could not be located; instead, a transition state with a substantially higher activation energy (52.2 kcal/mol) gives rise to **13** from **12**. The activation barrier increases to 56.2 kcal/mol (Table S2) at 393.15 K. Complex **13** can then give rise to NH_3 and H_2O with NH_4^+ in a similar manner to the transformation of **10** to **11** in Figure 3.

CONCLUSIONS

A well-defined and water-soluble Cu(II) complex, tetraammineaquacopper(II) sulfate, catalyzes urea formation from ammonium carbamate, which can be made from CO_2 and NH_3. The reaction does not require supercritical conditions. The reaction can be conducted in an aqueous solution, and the amount of water in the reaction mixture drastically affects the yield. An 18 ± 6% yield of urea was obtained in the presence of 28.9 ± 3.2 μL of water at 120 °C over 15 h. Up to 75 catalyst turnovers were obtained at 150 °C. Such yield and turnover were comparable to or better than the known catalytic urea synthesis carried out at or below 120 °C over 72 h.[5,19] The product urea was characterized using FT-IR, PXRD, and quantitative $^1H\{^{13}C\}$ NMR analyses. The catalyst was recovered at the end of the reaction in up to 70% recovery yield, verified by FT-IR, PXRD, and quantitative UV−vis analyses.

In computational studies, carbamic acid (as a transient intermediate) forms a complex with $[Cu(NH_3)_4]^{2+}$. The complex then undergoes a nucleophilic attack on the carbonyl of carbamic acid via an NH_3 ligand. As a result, the adduct intermediates **2**, **3**, and **4** are formed with a tetrahedral carbon moiety coordinated to Cu(II). These adduct intermediates have shallow minima on the potential energy surfaces. The proton transfer and the removal of the OH group lead to urea formation. To complete the catalytic cycle, a free NH_3 from the reaction mixture regenerates the catalyst $[Cu(NH_3)_4]^{2+}$ from either the $[Cu(urea)(NH_3)_3]^{2+}$ or $[Cu(H_2O)(NH_3)_3]^{2+}$ complex. Importantly, the formation of the adduct intermediates **2** and **4** is the key to low reaction barriers. The coordination of Cu(II) to the OH group of adduct intermediate **4** facilitates the removal of OH, giving a low reaction barrier of 2.0 kcal/mol from intermediate **4** (Figure 2). The Cu(II)-coordination with the carbonyl oxygen stabilizes adduct intermediates **2** and **4** so that one potentially high barrier is split into two low activation barriers to urea formation.

By DFT calculations, carbamate anion has lower complexation energy (by 5.85 kcal/mol) than carbamic acid to $[Cu(II)(NH_3)_4]^{2+}$, indicating that $[Cu(II)(NH_3)_4]^{2+}$-carbamate anion should be the starting point of the catalyzed reaction. However, no intermediate similar to **9** could be located with a carbamate anion (Figure S13), while intermediate **9** starting from $[Cu(NH_3)_4]^{2+}$-ammonium carbamate shows carbamic acid characteristics. Thus, carbamic acid can be involved as a transient intermediate in the catalytic conversion of carbamic ammonium to urea, even though the free carbamic acid is not stable at an ambient or elevated temperature.

EXPERIMENTAL PROCEDURE

General. Reagent-grade copper(II) sulfate pentahydrate, ammonium carbamate (99%), absolute ethanol (200 proof), aqueous ammonia solution (32 wt %), benzene, and DMSO-d_6 (deuterated dimethyl sulfoxide, >99%) were purchased from Sigma-Aldrich or VWR International. Tetraammineaquacopper(II) sulfate was purchased from Strem Chemicals and Sigma-Aldrich. The complex was also synthesized from copper sulfate pentahydrate using a method in the literature.[70] High-purity urea (>99%) was purchased from Duda Energy. CuO and Co_3O_4 powders were purchased from Sigma-Aldrich. Silicone heating oil, with a maximum operating temperature of 200 °C, was purchased from Fisher Scientific. Distilled water was used. Water in the catalytic reactions was delivered using either 0.5 mL or three drops of water with a 1 mL Norm-Ject disposable plastic syringe and a BD PrecisionGlide needle: gauge 22 and 1 in. An average mass of three drops of water, over seven measurements, was 28.9 ± 3.2 mg, which corresponds to 28.9 ± 3.2 μL.

Fourier Transform Infrared Spectroscopy (FT-IR). FT-IR analyses were performed using a Mattson Galaxy Series 3000 instrument. Samples for FT-IR were prepared by grinding in a mortar and pestle. The resulting powder mixture was analyzed via attenuated total reflectance (ATR) detector. The FT-IR spectra were collected from 600 to 4000 cm^{-1} and with a 1 cm^{-1} resolution.

FT-IR Spectroscopy of Complex 1. The FT-IR stretches of **Complex 1** in the literature[39] are N−H antisymmetric stretch: 3327 and 3253 cm^{-1}; N−H symmetric stretch: 3169 cm^{-1}; N−H bending modes: 1669, 1639, 1300, and 1283 cm^{-1}; and N−H rocking mode: 735 cm^{-1}.

Powder X-ray Diffraction (PXRD). A PXRD analysis was performed on a Rigaku Miniflex 600 instrument, equipped with a graphite crystal monochromator, a NaI scintillation counter detector, and a Cu Kα X-ray source. The goniometer has a minimum step width of 0.005 and an accuracy of 0.02. Data collection was performed under 40 kV and 15 mA (600 W). Qualitative and quantitative data analyses were conducted using a PDXL II software suite. The ICDD PDF4-mineral 2018−2019 database was used for phase indexing. A quantitative phase analysis of CuO was performed using a known amount of Co_3O_4 as an internal standard and the whole-pattern-

https://doi.org/10.1021/acs.inorgchem.0c03467
Inorg. Chem. 2021, 60, 5573−5589

profile-fitting (WPPF) and quantitative analysis features of a Rigaku PDXL II. Details of the instrument and the quantitative phase analysis are included in the Supporting Information.

The samples were ground using a mortar and pestle before analysis. Unless specified otherwise, 20−40 mg of powder was evenly spread across a 2 cm × 2 cm glass sample holder with a 0.2 or 0.5 mm indent, purchased from Rigaku. The sample was then pressed to a thin layer using a glass slide to form a flat surface. The data were collected from 15 to 80° 2θ with a scan rate of 2° 2θ per minute to analyze **Complex 1**. In the analysis of urea, the data were collected from 15 to 50° 2θ with a scan rate of 2° 2θ per minute for efficient analysis.

UV−Vis Spectroscopy of Complex 1. **Complex 1** was dissolved in a 1 M aqueous ammonia solution. The resulting solution has **Complex 1** at 4 mM. The UV−vis spectrum of the solution was obtained using a Cary 50 Bio spectrophotometer under wavelengths ranging from 300 to 800 nm at 23 °C. A band at λ_{max} = 605 nm was observed, assigned to the spin-allowed, d-to-d transition of the square-planar, d9 $[Cu(NH_3)_4]^{2+}$ complex. When using distilled water as the solvent without any NH_3, a minimum amount of water is used to avoid decomposition to $Cu(OH)_2$, a solid precipitate that is at equilibrium with **Complex 1**.[28]

High-Pressure Reactors. Urea synthesis from ammonium carbamate was conducted in 22 mL high-pressure metal reactors, purchased from Parr Instrument Company. They are made of a corrosion-resistant Hastelloy C-276 alloy. The maximum pressure is 1700 psi at 300 °C. All of the experiments were conducted under much milder conditions than the maximum: pressure of up to 300 psi and temperature up to 150 °C. The pressure was 50 psi at 120 °C for the reaction described in entry 1 in Table 1. Metal reactors made of T316 stainless steel were avoided because they often led to visible corrosion of the reactor via ammonium carbamate, leaching orange species that can catalyze the urea formation from ammonium carbamate.

Heating was then performed in either a drying oven or a heated silicone oil bath. The temperature was controlled and monitored using a thermometer or a thermal couple. The reaction pressure was monitored using a pressure gage integrated into a gage block assembly made by Parr Instrument Company.

CuO-Catalyzed Urea Formation. CuO in a 1% catalyst loading (0.26 mmol, 20 mg) and ammonium carbamate in 2.0 g (26 mmol) were added to a high-pressure metal reactor under air. An oven was preheated to 120 °C. The oven door was briefly opened, the high-pressure reactor was placed in the oven, and the oven door was quickly shut. The heating lasted for 3 days. Then, the oven was turned off and the door was opened to allow for cooling by air. The cooling took 30 min for the reactor to reach an ambient temperature (25−50 °C). The solid mixture containing the urea product was then dried under vacuum, with a liquid N_2 trap at 22 °C for 30 min to 1 h to remove the water side product.

The solid sample was then ground to a fine powder, which was stirred using a spatula to obtain a uniform sample. A 40 mg sample of the entire solid mixture was analyzed via $^1H\{^{13}C\}$ NMR spectroscopy (see the Quantitative Analysis of Urea Using Solution-Phase 1H{13C} NMR Spectroscopy section for details). Urea was detected at a 22% yield (5.6 mmol) based on the ammonium carbamate (26 mmol) starting material. The urea product after purification, via extraction with methanol, was confirmed by FT-IR and PXRD analyses (see the next section for details).

Purification by Extraction with Methanol. To analyze the urea product by FT-IR and PXRD spectroscopy, we purified urea using solid extraction via methanol. After the removal of water under vacuum for the reaction in the previous paragraph, the urea in the crude product mixture was extracted using 15 mL of methanol in a 50 mL centrifuge tube, followed by centrifugation at 3000 rpm for 3 min to separate the liquid from the solid. Vortexing was performed to ensure a thorough liquid−solid mixing. The solution of urea in methanol was then decanted into a 100 mL round-bottom flask, leaving the insoluble solid in the centrifuge tube. The methanol extraction was performed once more, and the solution was combined with the previous portion. The methanol was then removed under vacuum using a Rotavap at 45 °C for 30 min. The unreacted starting material, ammonium carbamate, was also present in the methanol solution, but it rapidly decomposed to CO_2 and NH_3, which were removed under vacuum. The dry powder was then analyzed by FT-IR and PXRD spectroscopy.

Catalytic Urea Synthesis Using Complex 1 in 0.5 mL of Water at 120 °C (Entry 1 in Table 1). **Complex 1** in a 1% catalyst loading (64 mg, 0.26 mmol), ammonium carbamate in 2.0 g (26 mmol), and water in 0.5 mL were added to a high-pressure metal reactor under air. The details of the syringe and needle are described in the General section.

An oven was preheated to 120 °C. The oven door was briefly opened, a high-pressure reactor was placed in the oven, and the oven door was shut quickly. The temperature in the oven dropped to 110 °C after placing the reactor. The heating lasted for 15 h, after which the oven was turned off and the door was opened to allow cooling by air. The cooling took 30 min for the reactor to reach an ambient temperature (25 °C). Urea at a 5% yield, based on ammonium carbamate, was obtained by $^1H\{^{13}C\}$ NMR analysis using benzene as an internal standard and in DMSO-d_6 (see the Quantitative Analysis of Urea Using Solution-Phase 1H{13C} NMR Spectroscopy section for details). The urea content was 90 ± 10% after purification by methanol extraction (see the Purification by Extraction with Methanol section for details). The purity was determined by comparing the total weight of the sample to the amount of urea measured using a quantitative $^1H\{^{13}C\}$ NMR analysis.

Powder X-ray Analyses of Urea and Biuret. The purified urea product was characterized by powder X-ray diffraction. Phase indexing was performed using the ICDD (The International Centre for Diffraction Data) PDF card of urea: 01-083-1436. The most intense reflections of urea appear at 22.19, 36.83, and 31.24° 2θ. All reflections matched those of urea. No significant biuret was detected.[36]

An attempt on the PXRD analysis of the potential side product, ammonium bicarbonate, was conducted for the reactions shown in entries 1 and 4 in Table 1. The analysis was performed after drying the crude product in vacuum for 30 min to 1 h and purification by extraction using methanol (see the Purification by Extraction with Methanol section for details). The PDF card of ammonium bicarbonate (teschemacherite), 00-044-1483, was used for phase indexing. The most intense reflections of ammonium bicarbonate appear at 16.75° 2θ. We could not determine whether ammonium bicarbonate is present because this reflection at 16.75° 2θ overlaps with the reflection of **Complex 1** at 16.77° 2θ. A PXRD spectrum of **Complex 1** is included in Figure S4 in the Supporting Information along with a list of reflections.

Catalyst Recovery and Spectroscopic Analyses. At the end of the reaction described in entry 1 in Table 1, the water was removed under vacuum and the solid was ground to a fine powder. Urea and ammonium carbamate in the crude product were removed via extraction using methanol (2 × 15 mL). A 50 mL centrifuge tube was used for the extraction. Vortexing was performed to ensure a thorough liquid−solid mixing. Centrifugation was performed at 3000 rpm for 3 min, and the supernatant was decanted.

The solid mixture, which is insoluble in methanol, consists of **Complex 1** and a white, solid impurity. The solid mixture was resuspended in 15 mL of methanol in a 50 mL centrifuge tube. The impurity has a large particle size and quickly precipitates at the bottom of the tube. The purple solids, **Complex 1**, are fine particles and are temporarily suspended in methanol. This solution suspension of **Complex 1** was decanted into a round-bottom flask, leaving behind the impurity at the bottom of the centrifuge tube. Upon solvent removal using a Rotavap, **Complex 1** was recovered and confirmed via FT-IR and PXRD spectroscopy.

Copper(II) Recovery by Precipitation with CO_2. At the end of the reaction described in entry 1 in Table 1, the product mixture was dissolved in 5 mL of water and transferred to a round-bottom flask. Water and ammonium carbamate were removed under vacuum with a liquid N_2 trap at 50 °C for 30 min. To thoroughly remove free NH_3 that can coordinate to copper(II), water in 5 mL was used to dissolve

https://doi.org/10.1021/acs.inorgchem.0c03467
Inorg. Chem. 2021, 60, 5573−5589

the product mixture again, followed by evaporation with liquid N_2 trap at 50 °C for another 30 min. Water in 5−10 mL was added to dissolve the solid, and CO_2 was vigorously bubbled into the solution for 3 min to precipitate copper(II) in the form of the basic copper carbonate ($Cu_2CO_3(OH)_2$). The cyan solid was filtered out and dried on a suction funnel at 23 °C for 30 min.

Catalytic Urea Formation by the Recovered Basic Copper Carbonate. The recovered basic copper carbonate (0.128 mmol or 28 mg of $Cu_2CO_3(OH)_2$) was used as a catalyst in 1% loading, based on copper(II), for urea synthesis in 0.5 mL of water at 120 °C over 15 h. Urea formed in a 2% yield, which was measured using quantitative $^1H\{^{13}C\}$ NMR spectroscopy with benzene (15 mg) as the internal standard. This reaction was carried out in an open glass vial (1.18 × 0.87 in, made by MaxMau) that was placed in a C-276 Hastelloy reactor to prevent corrosion from the metal reactor. Only the urea formed inside the glass vial was analyzed for the yield. Under otherwise identical conditions, **Complex 1** gave urea in a 4% yield.

UV−Vis Quantitation of the Recovered Complex 1. To quantify the recovered complex, the reaction, described in entry 1 in Table 1 was performed again. At the end of the reaction, water, urea, and ammonium carbamate were removed by drying in vacuum, methanol extraction (2 × 15 mL), and centrifugation, as described in the previous paragraph. The solid that is insoluble in methanol was dissolved in a 1 M aqueous ammonia solution to form a 10 mL solution using a volumetric flask. The absorption at λ_{max} = 605 nm was used to quantify **Complex 1**. A calibration plot was made using 10 mL solutions, which contained **Complex 1** in 0.008, 0.016, 0.024 M, and a blank sample, which contained only a 1 M aqueous ammonia solution. The molar absorptivity was 53.6 L mol^{-1} cm^{-1}, and the path length was 1 cm. The concentration of the recovered **Complex 1** was 0.0073 M, corresponding to a 29% recovery yield.

The recovery yield of **Complex 1** can be increased to 70% by the following procedure. At the end of the reaction described in entry 1 in Table 1, the product mixture was transferred to a round-bottom flask with the help of 5 mL of methanol. Water in this solution was thoroughly removed under vacuum at 50 °C with a liquid N_2 trap for 1 h. The resulting solid underwent methanol extraction (2 × 15 mL) and centrifugation to remove urea from **Complex 1**, as described in the Catalyst Recovery and Spectroscopic Analyses section. No insoluble white solid was observed in this extraction procedure. After the extraction, the remaining solid was dried under vacuum, dissolved in a 1 M aqueous ammonia solution, and analyzed by UV−vis spectroscopy.

Catalytic Urea Synthesis Using Complex 1, with 28.9 μL of Water, and at 120 °C (Entry 4 in Table 1). **Complex 1** in a 1% catalyst loading (64 mg, 0.26 mmol), ammonium carbamate in 2.0 g (26 mmol), and water in 28.9 ± 3.2 μL were added to a high-pressure metal reactor under air. The water was added via a syringe. The details of the syringe and needle are described in the General section.

An oven was preheated to 120 °C. The oven door was briefly opened, a high-pressure reactor was placed in the oven, and the oven door was shut quickly. The temperature in the oven dropped to 110 °C after placing the reactor. The heating lasted for 15 h, the oven was turned off, and the door was opened to allow cooling by air. The cooling took 30 min for the reactor to reach an ambient temperature (25 °C). Urea was detected at an 18 ± 6% yield, based on ammonium carbamate, using a $^1H\{^{13}C\}$ NMR analysis in DMSO-d_6, where benzene was an internal standard. The quantitative NMR analysis is described in the Quantitative Analysis 1H{13C} NMR Spectroscopy section.

UV−Vis Analysis of Copper(II) Biuret. At the end of the reaction described in entry 1 of Table 1, the product mixture was dissolved in water (5 mL). A 1 mL portion of this solution was diluted to 2 mL and analyzed by UV−vis spectroscopy. No absorption for copper biuret at 540 nm was detected.[35]

Quantitative Analysis of Urea Using Solution-Phase $^1H\{^{13}C\}$ NMR Spectroscopy. A Varian 400 MHz or an Anasazi 60 MHz NMR spectrometer was used for the quantitative $^1H\{^{13}C\}$ analysis of urea. The data processing was performed using ACD Spectrus Processor software. At the end of the reaction described in the previous paragraph and in entry 4 in Table 1, the solid mixture containing the urea product was dried under vacuum for 30 min to 1 h to remove the water. The sample was then ground to a fine powder and stirred using a spatula to obtain a uniform sample. The solid after drying and grinding has a total mass of 1440 mg. A 42.6 mg portion of the total sample was dissolved in 0.75 mL DMSO-d_6 and analyzed by $^1H\{^{13}C\}$ NMR spectroscopy.

Benzene, an internal standard in 8.9 mg, was then added to the DMSO-d_6 solution. The solution was analyzed using $^1H\{^{13}C\}$ NMR spectroscopy with the six equivalent proton signals of benzene, referenced at 7.33 ppm. The broad chemical shift at 5.49 ppm was assigned to the four N−H equivalent hydrogen atoms of urea. The urea was detected at a 24% yield (6.2 mmol) based on the starting ammonium carbamate material (26 mmol). No significant amount (>1%) of any other organic product was detected. The experiment was conducted thrice to obtain an average yield of 18 ± 6%. The characterization and quantitation methods were validated by testing a purchased sample of urea in 40 mg.

Catalytic Urea Synthesis Using Complex 1 without Water at 150 °C (Entry 16 in Table 1). **Complex 1** in the 0.2% catalyst loading (12 mg, 0.051 mmol) and ammonium carbamate in 2.0 g (26 mmol) were added to a high-pressure metal reactor under air. An oven was preheated to 150 °C. The oven door was briefly opened, a high-pressure reactor was placed in the oven, and the oven door was shut quickly. The temperature in the oven dropped to 125−130 °C after placing the reactor, and it took 1 h for the temperature to increase to 150 °C. The heating lasted for 17 h, the oven was turned off, and the door was opened to allow cooling by air. The cooling took 30 min to 1 h for the reactor to reach an ambient temperature (25−50 °C). The solid mixture containing the urea product was then dried in vacuum for 30 min to 1 h to remove water, a side product.

The solid sample was then ground to a fine powder, which was stirred using a spatula to obtain a uniform sample. After drying and grinding, the solid has a total mass of 1147 mg, of which 40 mg of the sample was analyzed via $^1H\{^{13}C\}$ NMR spectroscopy (see the Quantitative Analysis of Urea Using Solution-Phase 1H{13C} NMR Spectroscopy section for details). Urea was detected at a 15% yield (3.84 mmol) based on the ammonium carbamate starting material (26 mmol), corresponding to 75 catalyst turnovers. The experiment was reproducible. The turnovers were calculated by dividing the yield of the urea by the catalyst loading.

Synthesis of Tetraammineaquacopper(II) Sulfate (Complex 1). **Complex 1** was synthesized using a literature method,[70] where copper(II) sulfate pentahydrate and excess aqueous ammonia were combined, followed by precipitation by alcohol at 0 °C. The product was purified by washing with ethanol and pentane. The synthesis is highly reproducible. A purchased sample from Strem Chemicals was also used for catalysis. A PXRD spectrum of this complex, along with a list of reflections, is included on page 10 of the Supporting Information.

Calculation Methods. All structures are optimized at the B3LYP/6-31G** level of theory[71,72] with an SMD-water continuum solvent model,[73] and the frequencies are calculated at the same level to confirm that the structures are either minima (no imaginary frequencies) or transition states (only one imaginary frequency). The intrinsic reaction coordinate (IRC) method was employed to follow the forward and reverse reaction paths for every transition state, so that the corresponding reactants and products are identified.[74] All calculations are done with the Gaussian program package. In section 3.2, the Gibbs free energies are additionally estimated with single-point calculations at the M062x/6-311++G(3df,2pd) + SMD-water level of theory,[75] which is denoted as M062x/6-311++G(3df,2pd)//B3LYP/6-31G** + SMD-water. The sign "//" means "using the optimized structures of". The DFT calculations with both B3LYP and M062x are done with the unrestricted formula, UB3LYP or UM062X. The Mulliken spin density on Cu(II) is ∼0.74 in all species, and the spin densities are predominantly localized on Cu(II). The SMD solvent method was specifically developed to predict free energies of solvation by using

https://doi.org/10.1021/acs.inorgchem.0c03467
Inorg. Chem. 2021, 60, 5573−5589

different values for the radii and nonelectrostatic terms from the default SCRF model.[73]

■ ASSOCIATED CONTENT

Supporting Information

The Supporting Information is available free of charge at https://pubs.acs.org/doi/10.1021/acs.inorgchem.0c03467.

Details of the DFT calculations, a PXRD spectrum of **Complex 1**, FT-IR spectra of $Cu_2CO_3(OH)_2$, and the PXRD quantitative analysis of the recovered CuO (PDF)

■ AUTHOR INFORMATION

Corresponding Authors

Dequan Xiao − *Center for Integrative Materials Discovery, Department of Chemistry and Chemical Engineering, University of New Haven, West Haven, Connecticut 06516, United States;* orcid.org/0000-0001-6405-9106; Email: dxiao@newhaven.edu

Meng Zhou − *Department of Natural Sciences, Lawrence Technological University, Southfield, Michigan 48075, United States;* orcid.org/0000-0003-2524-8857; Email: mzhou@ltu.edu

Authors

Danielle S. Hanson − *Department of Natural Sciences, Lawrence Technological University, Southfield, Michigan 48075, United States*

Yigui Wang − *Center for Integrative Materials Discovery, Department of Chemistry and Chemical Engineering, University of New Haven, West Haven, Connecticut 06516, United States*

Xinrui Zhou − *Department of Natural Sciences, Lawrence Technological University, Southfield, Michigan 48075, United States*

Erik Washburn − *Department of Natural Sciences, Lawrence Technological University, Southfield, Michigan 48075, United States*

Merve B. Ekmekci − *Department of Natural Sciences, Lawrence Technological University, Southfield, Michigan 48075, United States*

Donovan Dennis − *Department of Natural Sciences, Lawrence Technological University, Southfield, Michigan 48075, United States*

Amay Paripati − *Department of Natural Sciences, Lawrence Technological University, Southfield, Michigan 48075, United States*

Complete contact information is available at: https://pubs.acs.org/10.1021/acs.inorgchem.0c03467

Funding

The authors thank the Lawrence Technological University for the Seed Grant in 2017. E.W. and M.Z. thank the Lawrence Technological University for the Presidential Undergraduate Research Award in 2018. D.X. thanks the "University Research Scholar Award" and "Endowed Jacob F. Buckman Chair Fund" from the University of New Haven and the research fund from the Higasket research fund.

Notes

The authors declare no competing financial interest.

■ ACKNOWLEDGMENTS

The authors thank the staff at the Lumigen Facilities at Wayne State University for the access to a 400 MHz NMR spectrometer. The calculations used the Extreme Science and Engineering Discovery Environment (XSEDE),[76] which is supported by the National Science Foundation Grant no. ACI-1053575. M.Z. thanks Robert H. Crabtree at Yale University for helpful discussions.

■ REFERENCES

(1) Meessen, J. H.; Petersen, H. Y. Urea. *Ullmann's Encyclopedia of Industrial Chemistry*; Wiley-VCH: Weinheim, 2000.

(2) Dallet, P.; Labat, L.; Kummer, E.; Dubost, J. P. Determination of Urea, Allantoin and Lysine Pyroglutamate in Cosmetic Samples by Hydrophilic Interaction Chromatography. *J. Chromatogr. B* **2000**, *742*, 447−452.

(3) Barzagli, F.; Mani, F.; Peruzzini, M. Carbon Dioxide Uptake as Ammonia and Amine Carbamates and Their Efficient Conversion into Urea and 1,3-Disubstituted Ureas. *J. CO_2 Util.* **2016**, *13*, 81−89.

(4) Müller, T. E. Opportunities for Utilizing and Recycling CO_2. In *Carbon Capture, Storage and Use: Technical, Economic, Environmental and Societal Perspectives*; Kuckshinrichs, W.; Hake, J., Eds.; Springer International: Cham, Heidelberg, New York, Dordrecht, and London, 2014; pp 67−100.

(5) Barzagli, F.; Mani, F.; Peruzzini, M. From Greenhouse Gas to Feedstock: Formation of Ammonium Carbamate from CO_2 and NH_3 in Organic Solvents and Its Catalytic Conversion into Urea under Mild Conditions. *Green Chem.* **2011**, *13*, 1267−1274.

(6) Omae, I. Recent Developments in Carbon Dioxide Utilization for the Production of Organic Chemicals. *Coord. Chem. Rev.* **2012**, *256*, 1384−1405.

(7) Tsipis, C. A.; Karipidis, P. A. Mechanistic Insights into the Bazarov Synthesis of Urea from NH_3 and CO_2 Using Electronic Structure Calculation Methods. *J. Phys. Chem. A* **2005**, *109*, 8560−8567.

(8) Suehiro, Y.; Nakajima, M.; Yamada, K.; Uematsu, M. Critical Parameters of $\{xCO_2 + (1- x) CHF_3\}$ for x=(1.0000, 0.7496, 0.5013, and 0.2522). *J. Chem. Thermodyn.* **1996**, *28*, 1153−1164.

(9) Brunner, E. Fluid Mixtures at High Pressures VI. Phase Separation and Critical Phenomena in 18 (N-Alkane + Ammonia) and 4 (N-Alkane + Methanol) Mixtures. *J. Chem. Thermodyn.* **1988**, *20*, 273−297.

(10) Durisch, W.; Lemkowitz, S. M.; van den Berg, P. J. Constituent and Component Measurements and Calculations of the Vapour/Liquid Equilibrium of the Ternary System Carbon Dioxide-Ammonia-Water under Urea Synthesis Conditions. *Chimia* **1980**, *34*, 314−322.

(11) Piotrowski, J.; Kozak, R.; Kujawska, M. Thermodynamic Model of Chemical and Phase Equilibrium in the Urea Synthesis Process. *Chem. Eng. Sci.* **1998**, *53*, 183−186.

(12) Bagnell, L.; Hodges, A.; Linton, M.; Mau, A. A New Equilibrium Model for the Bazarov Urea Synthesis Process. *Aust. J. Chem.* **1989**, *42*, 1819−1829.

(13) Claudel, B.; Brousse, E.; Shehadeh, G. Novel Thermodynamic and Kinetic Investigation of Ammonium Carbamate Decomposition into Urea and Water. *Thermochim. Acta* **1986**, *102*, 357−371.

(14) Gorlovskii, D.; Kucheryavyi, V. Equation for Determination of the Equilibrium Degree of CO_2 Conversion During Synthesis of Urea. *J. Appl. Chem. USSR* **1980**, *53*, 1898−1900.

(15) Inoue, S.; Kanai, K.; Otsuka, E. Equilibrium of Urea Synthesis. I. *Bull. Chem. Soc. Jpn.* **1972**, *45*, 1339−1345.

(16) Inoue, S.; Kanai, K.; Otsuka, E. Equilibrium of Urea Synthesis. II. *Bull. Chem. Soc. Jpn.* **1972**, *45*, 1616−1619.

(17) Yahya, N.; Qureshi, S.; Rehman, Z. U.; Alqasem, B.; Fai Kait, C. Green Urea Synthesis Catalyzed by Hematite Nanowires in Magnetic Field. *J. Magn. Magn. Mater.* **2017**, *428*, 469−480.

(18) Shi, F.; Deng, Y.; SiMa, T.; Peng, J.; Gu, Y.; Qiao, B. Alternatives to Phosgene and Carbon Monoxide: Synthesis of

Symmetric Urea Derivatives with Carbon Dioxide in Ionic Liquids. *Angew. Chem., Int. Ed.* **2003**, *42*, 3257−3260.
(19) Manaka, Y.; Nagatsuka, Y.; Motokura, K. Organic Bases Catalyze the Synthesis of Urea from Ammonium Salts Derived from Recovered Environmental Ammonia. *Sci. Rep.* **2020**, *10*, No. 2834.
(20) Crabtree, R. H. Alkane C−H Activation and Functionalization with Homogeneous Transition Metal Catalysts: A Century of Progress−a New Millennium in Prospect. *J. Chem. Soc., Dalton Trans.* **2001**, 2437−2450.
(21) Kumar, A.; Bhatti, T. M.; Goldman, A. S. Dehydrogenation of Alkanes and Aliphatic Groups by Pincer-Ligated Metal Complexes. *Chem. Rev.* **2017**, *117*, 12357−12384.
(22) Janowicz, A. H.; Bergman, R. G. Carbon−Hydrogen Activation in Completely Saturated Hydrocarbons: Direct Observation of M + R−H → M(R)(H). *J. Am. Chem. Soc.* **1982**, *104*, 352−354.
(23) Krishnakumar, V.; Chatterjee, B.; Gunanathan, C. Ruthenium-Catalyzed Urea Synthesis by N−H Activation of Amines. *Inorg. Chem.* **2017**, *56*, 7278−7284.
(24) Lane, E. M.; Hazari, N.; Bernskoetter, W. H. Iron-Catalyzed Urea Synthesis: Dehydrogenative Coupling of Methanol and Amines. *Chem. Sci.* **2018**, *9*, 4003−4008.
(25) Dobereiner, G. E.; Crabtree, R. H. Dehydrogenation as a Substrate-Activating Strategy in Homogeneous Transition-Metal Catalysis. *Chem. Rev.* **2010**, *110*, 681−703.
(26) Bjerrum, J.; Ballhausen, C. J.; Jorgensen, C. K. Studies on Absorption Spectra. *Acta Chem. Scand.* **1954**, *8*, 1275−1289.
(27) Schäffer, C. E. Jannik Bjerrum (1909−1992). *ACS Symp. Ser.* **1994**, *565*, 96−114.
(28) Johnson, A. R.; McQueen, T. M.; Rodolfa, K. T. Species Distribution Diagrams in the Copper-Ammonia System: An Updated and Expanded Demonstration Illustrating Complex Equilibria. *J. Chem. Educ.* **2005**, *82*, No. 408.
(29) Nilsson, K. B.; Eriksson, L.; Kessler, V. G.; Persson, I. The Coordination Chemistry of the Copper (II), Zinc (II) and Cadmium (II) Ions in Liquid and Aqueous Ammonia Solution, and the Crystal Structures of Hexaamminecopper (II) Perchlorate and Chloride, and Hexaamminecadmium (II) Chloride. *J. Mol. Liq.* **2007**, *131*, 113−120.
(30) Elliott, H.; Hathaway, B. The Hexaammine Complexes of the Copper (II) Ion. *Inorg. Chem.* **1966**, *5*, 885−889.
(31) Hathaway, B.; Tomlinson, A. Copper (II) Ammonia Complexes. *Coord. Chem. Rev.* **1970**, *5*, 1−43.
(32) Valli, M.; Matsuo, S.; Wakita, H.; Yamaguchi, T.; Nomura, M. Solvation of Copper (II) Ions in Liquid Ammonia. *Inorg. Chem.* **1996**, *35*, 5642−5645.
(33) Martell, A. E.; Hancock, R. D. *Metal Complexes in Aqueous Solutions*; Springer US: New York, 1996.
(34) Miessler, G. L.; Fischer, P. J.; Tarr, D. A. *Inorganic Chemistry*, 5th ed.; Pearson: Boston, 2014.
(35) Hortin, G. L.; Meilinger, B. Cross-Reactivity of Amino Acids and Other Compounds in the Biuret Reaction: Interference with Urinary Peptide Measurements. *Clin. Chem.* **2005**, *51*, 1411−1419.
(36) Wang, M.-L.; Zhong, G.-Q.; Chen, L. Synthesis, Optical Characterization, and Thermal Decomposition of Complexes Based on Biuret Ligand. *Int. J. Opt.* **2016**, *2016*, No. 5471818.
(37) Li, Z.; Zhang, B. Experimental and Theoretical Investigation of Homogeneous Gaseous Reaction of $CO_2(g)$ + $nH_2O(g)$ + $nNH_3(g)$ → Products (n = 1, 2). *J. Phys. Chem. A* **2012**, *116*, 8989−9000.
(38) Trevani, L. N.; Roberts, J. C.; Tremaine, P. R. Copper(II)−Ammonia Complexation Equilibria in Aqueous Solutions at Temperatures from 30 to 250 °C by Visible Spectroscopy. *J. Solution Chem.* **2001**, *30*, 585−622.
(39) Nakamoto, K. Applications in Coordination Chemistry. In *Infrared and Raman Spectra of Inorganic and Coordination Compounds*; Nakamoto, K., Ed.; John Wiley & Sons: Hoboken, 2008.
(40) Conley, R. T. *Infrared Spectroscopy*, 2nd ed.; Allyn & Bacon: Boston, 1972.
(41) Glemser, O.; Sauer, H. Basic Copper Carbonates. In *Handbook of Preparative Inorganic Chemistry*; Brauer, G., Ed.; Academic Press: New York, 1965; Vol. 2, pp 1024−1025.
(42) Watson, C. J. Assessment of Granular Urea/ammonium Sulphate and Urea/Potassium Nitrate Fertilizers on Nitrogen Recovery by Ryegrass. *Fertil. Res.* **1988**, *18*, 19−29.
(43) Gualtieri, A.; Viani, A.; Montanari, C. Quantitative Phase Analysis of Hydraulic Limes Using the Rietveld Method. *Cem. Concr. Res.* **2006**, *36*, 401−406.
(44) David, W. I. F.; Baerlocher, C.; McCusker, L. B.; Shankland, K. *Structure Determination from Powder Diffraction Data*; Oxford University Press: Oxford, 2002.
(45) Rietveld, H. A Profile Refinement Method for Nuclear and Magnetic Structures. *J. Appl. Crystallogr.* **1969**, *2*, 65−71.
(46) Zhou, X.; Liu, D.; Bu, H.; Deng, L.; Liu, H.; Yuan, P.; Du, P.; Song, H. XRD-Based Quantitative Analysis of Clay Minerals Using Reference Intensity Ratios, Mineral Intensity Factors, Rietveld, and Full Pattern Summation Methods: A Critical Review. *Solid Earth Sci.* **2018**, *3*, 16−29.
(47) Tsipis, C. A.; Karipidis, P. A. Mechanism of a Chemical Classic: Quantum Chemical Investigation of the Autocatalyzed Reaction of the Serendipitous Wöhler Synthesis of Urea. *J. Am. Chem. Soc.* **2003**, *125*, 2307−2318.
(48) Adams, J. M.; Small, R. W. H. The Crystal Structure of Ammonium Carbamate. *Acta Crystallogr. B* **1973**, *29*, 2317−2319.
(49) Crabtree, R. H. Hypervalency, Secondary Bonding and Hydrogen Bonding: Siblings under the Skin. *Chem. Soc. Rev.* **2017**, *46*, 1720−1729.
(50) Aresta, M.; Ballivet-Tkatchenko, D.; Dell'Amico, D. B.; Bonnet, M. C.; Boschi, D.; Calderazzo, F.; Faure, R.; Labella, L.; Marchetti, F. Isolation and Structural Determination of Two Derivatives of the Elusive Carbamic Acid. *Chem. Commun.* **2000**, *13*, 1099−1100.
(51) Ramachandran, B. R.; Halpern, A. M.; Glendening, E. D. Kinetics and Mechanism of the Reversible Dissociation of Ammonium Carbamate: Involvement of Carbamic Acid. *J. Phys. Chem. A* **1998**, *102*, 3934−3941.
(52) Johnson, S. L.; Morrison, D. L. Kinetics and Mechanism of Decarboxylation of N-Arylcarbamates. Evidence for Kinetically Important Zwitterionic Carbamic Acid Species of Short Lifetime. *J. Am. Chem. Soc.* **1972**, *94*, 1323−1334.
(53) Dell'Amico, D. B.; Calderazzo, F.; Farnocchi, S.; Labella, L.; Marchetti, F. The NHR_2/CO_2 System as a Metal Ion Extraction Reagent from Aqueous Solution into Hydrocarbons: Copper(II) and Zinc(II). *Inorg. Chem. Commun.* **2002**, *5*, 848−852.
(54) Khanna, R. K.; Moore, M. H. Carbamic Acid: Molecular Structure and IR Spectra. *Spectrochim. Acta A* **1999**, *55*, 961−967.
(55) Bresciani, G.; Biancalana, L.; Pampaloni, G.; Marchetti, F. Recent Advances in the Chemistry of Metal Carbamates. *Molecules* **2020**, *25*, No. 3603.
(56) Olah, G. A.; Heiner, T.; Rasul, G.; Prakash, G. K. S. ^{1}H, ^{13}C, ^{15}N NMR and Theoretical Study of Protonated Carbamic Acids and Related Compounds1. *J. Org. Chem.* **1998**, *63*, 7993−7998.
(57) Yu, J.; Chuang, S. S. C. The Role of Water in CO_2 Capture by Amine. *Ind. Eng. Chem. Res.* **2017**, *56*, 6337−6347.
(58) Pavelka, M.; Burda, J. V. Theoretical Description of Copper Cu(I)/Cu(II) Complexes in Mixed Ammine-Aqua Environment. DFT and Ab Initio Quantum Chemical Study. *Chem. Phys.* **2005**, *312*, 193−204.
(59) Morosin, B. The Crystal Structures of Copper Tetrammine Complexes. A. $Cu(NH_3)_4SO_4{\cdot}H_2O$ and $Cu(NH_3)_4SeO_4$. *Acta Crystallogr. B* **1969**, *25*, 19−30.
(60) Rojas-Hernández, A.; Ramírez, M. T.; González, I.; Ibáñez, J. G. Predominance-Zone Diagrams in Solution Chemistry: Dismutation Processes in Two-Component Systems (M−L). *J. Chem. Educ.* **1995**, *72*, No. 1099.
(61) Rayner-Canham, G.; Overton, T. *Descriptive Inorganic Chemistry*, 6th ed.; Macmillan: New York, 2009.
(62) Luther, G. W. *Inorganic Chemistry for Geochemistry and Environmental Sciences: Fundamentals and Applications*; Wiley: Chichester, 2016.
(63) Halpern, J. Mechanism and Stereoselectivity of Asymmetric Hydrogenation. *Science* **1982**, *217*, 401−407.

https://doi.org/10.1021/acs.inorgchem.0c03467
Inorg. Chem. 2021, 60, 5573−5589

(64) Zhou, M.; Johnson, S. I.; Gao, Y.; Emge, T. J.; Nielsen, R. J.; Goddard, W. A.; Goldman, A. S. Activation and Oxidation of Mesitylene C−H Bonds by (Phebox)Iridium(III) Complexes. *Organometallics* **2015**, *34*, 2879−2888.
(65) Watson, A. J. A.; Williams, J. M. J. The Give and Take of Alcohol Activation. *Science* **2010**, *329*, 635.
(66) Longwitz, L.; Werner, T. The Mitsunobu Reaction, Reimagined. *Science* **2019**, *365*, 866−867.
(67) Yamamoto, H.; Pandey, G.; Asai, Y.; Nakano, M.; Kinoshita, A.; Namba, K.; Imagawa, H.; Nishizawa, M. Catalytic Activation of the Leaving Group in the S_N2 Reaction. *Org. Lett.* **2007**, *9*, 4029−4032.
(68) Pearson, R. G. Hard and Soft Acids and Bases, HSAB, Part 1: Fundamental Principles. *J. Chem. Educ.* **1968**, *45*, No. 581.
(69) Bramsen, F.; Bond, A. D.; McKenzie, C. J.; Hazell, R. G.; Moubaraki, B.; Murray, K. S. Self-Assembly of the Octanuclear Cluster $[Cu_8(OH)_{10}(NH_2(CH_2)_2CH_3)_{12}]^{6+}$ and the One-Dimensional N-Propylcarbamate-Linked Coordination Polymer $\{[Cu(O_2CNH(CH_2)_2CH_3)(NH_2(CH_2)_2CH_3)_3](ClO_4)\}_n$. *Chem. - Eur. J.* **2005**, *11*, 825−831.
(70) Glemser, O.; Sauer, H. Tetraamminecopper (II) Sulfate. In *Handbook of Preparative Inorganic Chemistry*; Brauer, G., Ed.; Academic Press: New York, 1965; Vol. 2, pp 1021.
(71) Becke, A. D. Density-Functional Thermochemistry. III. The Role of Exact Exchange. *J. Chem. Phys.* **1993**, *98*, 5648−5652.
(72) Lee, C.; Yang, W.; Parr, R. G. Development of the Colle-Salvetti Correlation-Energy Formula into a Functional of the Electron Density. *Phys. Rev. B* **1988**, *37*, 785−789.
(73) Marenich, A. V.; Cramer, C. J.; Truhlar, D. G. Universal Solvation Model Based on Solute Electron Density and on a Continuum Model of the Solvent Defined by the Bulk Dielectric Constant and Atomic Surface Tensions. *J. Phys. Chem. B* **2009**, *113*, 6378−6396.
(74) Foresman, J. B.; Frisch, A. E. *Exploring Chemistry with Electronic Structure Methods*, 3rd ed.; Gaussian, Inc.: Wallingford, CT, 2015.
(75) Zhao, Y.; Truhlar, D. G. The M06 Suite of Density Functionals for Main Group Thermochemistry, Thermochemical Kinetics, Noncovalent Interactions, Excited States, and Transition Elements: Two New Functionals and Systematic Testing of Four M06-Class Functionals and 12 Other Functionals. *Theor. Chem. Acc.* **2008**, *120*, 215−241.
(76) Towns, J.; Cockerill, T.; Dahan, M.; Foster, I.; Gaither, K.; Grimshaw, A.; Hazlewood, V.; Lathrop, S.; Lifka, D.; Peterson, G. D.; Roskies, R.; Scott, J. R.; Wilkins-Diehr, N. XSEDE: Accelerating Scientific Discovery. *Comput. Sci. Eng.* **2014**, *16*, 62−74.

https://doi.org/10.1021/acs.inorgchem.0c03467
Inorg. Chem. 2021, 60, 5573−5589